712

Fermilab Proposal No.
Spokesperson: P. Rapp
Fermilab
Phone: (312) 840-4107
FTS 370-4107

STUDY OF MUONS FROM $\bar{P}P$ COLLISIONS UP TO $\sqrt{s}$ = 2 TeV

Dan Green, Herman Haggerty, Ernest Malamud, and Pat Rapp

Fermilab

and

Robert Ellsworth

George Mason University

February 1, 1982

Abstract

We propose a simple, moderate cost apparatus for detection of single and multiple muons emerging from the D0 colliding region. The copious background muon sources inherent in general purpose detectors suggest a special purpose closed-geometry detection scheme. The detector has two wire-wound steel spectrometers, each subtending $45^{\circ} < \theta < 135^{\circ}$ and $\Delta\phi = \pi/2$. The steel is close to the beam to minimize pion decay and it is thick to minimize punchthrough as well as provide a substantial muon momentum threshold. A large array of aboveground scintillators allows a clean elimination of the cosmic ray background. Rates, spectra, and charge ratios will be measured as a function of $\sqrt{s}$ for $P_{t\mu} \geq 3.6$ GeV/c. This is a straightforward and powerful method to search for new phenomena.

Following CDF we base our rate estimates on a run of integrated luminosity $10^{36}cm^{-2}$ or $10^{30}cm^{-2}sec^{-1}$ for 300 hours.

Contents

Physics Motivation

Introduction

The CDF group has done an elegant and thorough job of outlining the overall motivation for studying collisions at $\sqrt{s}$ = 2 TeV.[1] Our feeling is that a general purpose detector must make compromises. In particular, the physics inherent in prompt muon detection is of such interest as to make the optimal design of a special purpose closed-geometry muon detector attractive. What we propose here is basically a beam dump experiment. The experiment has been designed to study only the direct production of high P_t muons. The magnetized steel spectrometers which limit decay and hadronic punchthrough also provide a P_t cutoff which removes most of the copious known sources of prompt muons.

One of the known sources of prompt muons is heavy flavor production: $\bar{D}D, \psi$, $\bar{B}B, \Upsilon$. The detector P_t cutoff will largely eliminate these sources, leaving the experiment sensitive only to postulated heavy flavors. For example, $\bar{T}T$ production with a top quark mass of 20 GeV would yield muons with enough P_t to trigger the apparatus with detectable rates.

The apparatus is, of course, well matched to detecting electroweak bosons. One expects that muons from leptonic $W^{\pm}$ decays will have $P_t \sim M_W/2 \sim 40$ GeV/c. One also expects that the yield will be rapidly rising as $\sqrt{s}$ increases. Similarly, Z^0 will yield dimuons with detectable rates at large P_t and with strong $\sqrt{s}$ dependence. These rates are, however, still rather low in comparison to background sources. In particular $\pi \rightarrow \mu\nu$ decay and hadronic punchthrough must be minimized if the signal is to exceed the background.

Finally, one is pushing back the energy frontier. That is exciting, important, and, given some luck, could yield unexpected discoveries. A heavy object with mass $M_x > 200$ GeV is expected to be contained within our apparatus, $|y| < 1$. For a total luminosity of 10^{36} cm^{-2}, at the 10 event level we will be sensitive to very heavy objects X if $\sigma(x)B(x\rightarrow\mu) > 2 \times 10^{-35} cm^{-2}$.

Heavy Flavor Production

Heavy flavors will yield prompt muons. The cross sections for $\bar{D}D, \psi$, $\bar{B}B$, and $\bar{T}T$ are taken from a gluon fusion model.[2] Semileptonic branching ratios have been taken either from data (D and ψ) or from color counting arguments (B and T). Assuming a top quark mass of 20 GeV and an integrated luminosity of 10^{36} cm^{-2}, our apparatus acceptance ($\Delta\phi = \pi$, $|y|$

<1) then leads to the yields as a function of $\sqrt{s}$ shown in Fig. 1. The rapidity acceptance has been estimated[3] to reduce the rate by $\epsilon(y) \sim 0.2$.

The P_t cutoff (2.1, 3.6 GeV/c) has a dramatic effect on the muon yield from heavy flavors. This effect is rather model dependent since the dynamics of both heavy flavor production and decay are uncertain. Gluon fusion models for production[4] indicate that $d\sigma/dk_t^2 \sim e^{-A(k_t^2+M^2)^{1/2}}$ with $A \sim 3$ GeV^{-1}. Since this distribution has a maximum at $k_{tmax} = M/(A^2 - 1)^{1/2} \sim 0.35$ M, one expects heavier objects to be produced with larger k_t, the scale being set by $k_t \sim M$. However, for a 3-body semileptonic decay this production k_t is washed out: $M \rightarrow \mu\nu X$ gives $\langle P_t \rangle \sim 1/3(k_t^2 + M^2)^{1/2}$. This naive argument is confirmed by detailed Monte Carlo calculations.[5]

The P_t cutoff of 3.6 GeV/c, assuming a gluon fusion model and 3-body semileptonic decay, means that the up trigger is sensitive only to masses M > 10 GeV. This means that we are insensitive to all the "old" physics, $\bar{D}D$, ψ, $\bar{B}B$. For example, assuming a top quark mass of 20 GeV and letting $\epsilon(P_t) = 1/2$ represent the effect of the P_t cutoff, the rate for a "standard run" (10^{36}) is 800 muons above 3.6 GeV/c due to T decays. The P_t spectrum will be distinctive of T decays. One also expects that the yield will rise by an order of magnitude for $\sqrt{s}$ rising from 0.4 TeV to 2.0 Tev, which will also be indicative. If the top quark mass were 60 GeV the yield would be at the sensitivity limit of 10

events.[6]

Electroweak Boson Production

Direct observation of the gauge bosons is crucial to the SU(2)xU(1) electroweak theory. The standard theory predicts substantial cross sections[7] for $W^{\pm}$ and Z^0 masses of 83 and 93 GeV, widths $\sim$3 GeV, and muonic branching ratios of 8% and 3%, respectively. The rapidity range is limited[8] such that for our detector $\mathcal{E}(y) \sim 0.5$, 0.3, respectively. The 30% figure for the Z^0 is the rapidity range efficiency for catching both muons.[8] The P_t spectrum is such that $\mathcal{E}(P_t) \sim 1.0$. We have used the same model as CDF to facilitate comparisons.

Given these assumptions, the expected rates as a function of $\sqrt{s}$ are shown in Fig. 2. At $\sqrt{s}$ = 2 TeV the signal is clearly detectable: 500 single muons from W's and 80 muon pairs from Z's into the apparatus for a standard run. The $\sqrt{s}$ dependence may be distinctive as the cross sections vary by an order of magnitude from $\sqrt{s}$ = 0.6 to $\sqrt{s}$ = 2.0 TeV.

The $\mu^{\pm}$ asymmetry due to parity violation[9] is another signature for $W^{\pm}$ production in addition to the $\sqrt{s}$ dependence and the peak in the P_t spectrum. Clearly this signature is inaccessible to experiments using non-magnetic $e^{\pm}$ detection techniques.

Of course these low rates are susceptible to backgrounds. Real prompt muon backgrounds from heavy flavors and the Drell-Yan continuum are expected to be negligible at $P_t \sim M_W/2 \sim 40$ GeV. From the previous discussion of heavy flavors one expects 800 muons above 3.6 GeV/c, with a spectrum peaking at 6.7 GeV/c and falling rapidly to zero at $P_t \sim 20$ GeV/c. The Drell-Yan dimuon production dynamics can and will be studied, but with detectable rates out to only $P_t \sim 12$ GeV/c, corresponding to dimuon masses of ~ 25 GeV. The major backgrounds in this experiment, even after optimization, are still prosaic: cosmic rays, hadronic punchthrough, and decays in flight. As discussed below, if the Jacobian peak exists, then these backgrounds can be reduced to tolerable levels since the signal is localized at rather high P_t, $P_t \sim 40$ GeV/c.

Finally, a comment should be made about the Jacobian peak technique. In QCD the W is expected[10] to be produced with substantial k_t, with the scale set by M_W as alluded to in the heavy flavor discussion above. If this be the case then the peak is strongly smeared. Since the apparatus has a limited P_t resolution due to the necessity of a closed geometry to reduce backgrounds, it is relatively well matched to this smearing. Very crudely, $\langle P_t \rangle_\mu \sim 1/2|M_W + k_{tW}|$ so that if $k_{tW} = 0.35\ M_W$ the peak is smeared by up to $\pm 35\%$ in P_t. We regard such smearing as likely and place more emphasis on background rejection than on good momentum

resolution.

Heavy Particle Production

Massive particles, M > 200 GeV, will be inaccessible except at the FNAL collider for a long time. The discovery of any such heavy particle would doubtlessly have great impact on high energy physics.

Where is a good place to look? Kinematics and the composite nature of hadrons suggest that 90^{o} is the place to look. In Fig. 4 is shown the rapidity HWHM expected for heavy particles as a function of $\sqrt{s}$ using a gluon annihilation model, $d\sigma/dy \sim G(x_1) \cdot G(x_2)$. The plot shows that masses above 160 GeV are contained within the apparatus, $|y| < 1.0$.

As discussed above, one expects heavy objects to be produced with a P_t whose scale is set by the mass of the object: $P_t \sim 0.35$ M. As our apparatus sits at 90^{o} and subtends $|y| < 1.0$ with a momentum cutoff of 3.6 GeV/c, it largely tunes out the old physics and, hopefully, tunes in the new. Given a modest sized detector, i.e., not 4π, this location appears to be optimal.

The Apparatus

Introduction

The detector is a pair of magnetic spectrometers, one above and one below the $\bar{P}P$ interaction region. The two arms are sheltered under a cosmic ray umbrella consisting of two planes of scintillator, one on top of the up arm and the other above ground. (Fig. 4) The up and down arms trigger independently on single muons and have some reasonable efficiency for dimuons (Drell-Yan, Z's, X_{Heavy}). The two arms are identical except that the up arm incorporates the above-ground scintillator (SU3) into its trigger and therefore has a higher energy threshold for triggering muons.

The detector has been designed to fit in a transverse operating area 15 ft. on a side. (See the Alternative Configurations section) Longitudinally the arms taper from 11 ft. immediately above and below the beam to 22 ft. along the floor and ceiling. With this configuration the D0 area could be shared by both forward detectors and left/right detectors, which could stand on our down arm. A short-lifetime microvertex detector would mate naturally to our detector. These other users would certainly be welcome to the cosmic ray signal which we will provide.

The coordinate system used has the protons going toward positive Z. Positive Y is up and X is chosen to make a right-handed system. Θ and ϕ are the usual polar and azimuthal angles.

Spectrometer Magnets

The detector has two identical arms, one below and one above the interaction region. The down arm is shown in Fig. 5. It consists of three wire-wound Fe magnets, four wire-chamber tracking stations, and two scintillator triggering planes.

The magnetic field lines are horizontal and have a race track configuration. Non-magnetic spacers are placed between the sides of the race track so that they keep their distance. In each arm the outer pair of magnets share a common flux return to maintain the 22 ft^2 area occupied by the flux going through the windings. The result is to bend the ends of the horizontal race track toward the vertical. In this way we can keep $\Delta\theta = 90^{\circ}$ acceptance without extending the Fe more than 22 ft. Total weight of the Fe is 530 tons. In all cases the steel is supported under the ends, outside the windings. The up arm can be supported by non-magnetic posts sitting on the down arm.

All the fields are assumed to be only 14 KG so that the high permeability (~1000) keeps the field in the Fe. The resulting momentum kick is 0.76 Gev/cos λ , where all the bending is in the transverse (XY) plane and the helix pitch λ is related to the polar angle by $\lambda = |\theta - 90|$.

In the up arms holes are cut in all four flux returns to allow for passage of the present main ring beam pipe at 30 in. above the interaction region. Through most of the detector length that beam pipe will pass through the 6 in. gap between the sides of the smaller up magnet. The fields can be turned off, and even zeroed if necessary, during the time the main ring is being ramped.

Scintillator Trigger

Each arm has two planes of scintillator for triggering. The planes nearer the beam are called SU1 and SD1 where U (D) indicates the up (down) spectrometer arm. The planes further from the beam are called SU2 and SD2. Each of the four planes is divided into a right (R) and a left (L) half-plane. The trigger is the OR of the up trigger and the down trigger, given by

UPTRIG = SU1R·SU2R·SU3 + SU1L·SU2L·SU3, and

DNTRIG = SD1R·SD2R + SD1L·SD2L

Triggering in this way assures that the muon did not bend through reversed fields in getting to the outer scintillator.

In actual construction all half-planes (except SU2's) are made from 2 ft. wide slats of scintillator. The slats lie transverse to the beam. Each S1 half-plane has 6 slats, each 5 ft. long. Each SD2 half-plane has 8 slats, each 7 ft. long. The planes SU1, SD1, and SD2 require a total of 40 photomultiplier tubes.

The SU2 plane has a more sophisticated construction because of its participation in the cosmic ray veto. The scintillator slats are 8" x 8' and lie parallel to the beam line. The slats are overlapped as shown in Fig. 4. SU2 has a total of 48 slats. Phototubes are mounted on both ends for a total of 96 channels. Using end-to-end timing we expect a position resolution of ±8" longitudinally and ±4" transversely.

The SU3 plane is made of 16 liquid scintillator tanks, each 6 in. thick and 12 ft. x 12 ft. in area. Each tank is divided optically into 6 channels, each 2 ft. x 12 ft. Both ends are read out by tubes attached directly to the ends of each channel, a total of 192 tubes. The channels are oriented in the same direction as the slats in SU2; i.e., longitudinally. Position resolution is ±8" longitudinally and ±12" transversely. The tanks are filled after they are

in position. Removing them is quick and easy if they are first pumped out. This scheme will probably be necessary since SU3 is placed in the D0 staging area.

Scintillator area mismatch to the 2 in. phototubes is inconsequential. In each half-plane all the slats are 'ORED' together to make the half-plane signal for the trigger. The total number of tubes is 328. Of these 288 (SU3 and SU2) require ADC channels. The other 40 (SU1, SD1, and SD2) are latched only. In addition we need 6 ADC channels to record the summed signals from the SU1, SD1, and SD2 half-planes. The use of the 294 ADC channels in reducing cosmic and punchthrough backgrounds is discussed later in the section on backgrounds.

Tracking Chambers

Each spectrometer has four stations of wire chambers. The innermost stations are used together on all tracks to determine accurately the position of the interaction. At present we have not yet decided what type chambers to use for these innermost planes. The other six stations will be drift chambers, probably of the E613 type. They have 4" x 1" cells separated by I-beams and sheathed in 1/16 in. aluminum. Maximum drift time is 1 μs, which is comfortably less than the time between bunch crossings. Multi-hit capability can be provided. Position resolution

is 300 um, which is roughly half the displacement due to multiple scattering of a 100 GeV muon through 1/2 the spectrometer. Somewhere above 100 GeV/c the smearing due to multiple scattering gets smaller than the chamber resolution and the momentum resolution starts to degrade. For muons with $P_\mu < 100$ GeV/c the chambers do not contribute to the error and $\Delta P/P$ is determined by multiple scattering errors. For N measurements of positions x_i at depths y_i in the steel, with field B_o, we find

$$\Delta P/P \propto 1/\left[B_o \sqrt{\textstyle\sum_i y_i - N^2 \sum_i y_i^{-1}}\right]$$

Given the layout of Fig. 4, this gives $\Delta P/P = \pm 0.30$ at $B_o = 14$ KG. Given more space at D0 we could increase the steel thickness, with the resolution improving as $y^{-1/2}$. Using higher quality steel improves the resolution as B_o^{-1}. Free-space tracking of muons is untenable because of decay and punchthrough backgrounds, as will be discussed in the next section.

In any case the smearing of the $W \to \mu\nu$ Jacobian peak is likely to be roughly matched to our momentum resolution. For Z^o dimuons we expect $\Delta M/M \sim \frac{1}{\sqrt{2}} \Delta P/P$ or $\Delta M \sim \pm 20$ GeV at the Z^o mass which will preclude a measurement of the Z^o width. Nonetheless the Z^o signal should exceed the Drell-Yan background even with our poor momentum resolution.

The position resolution in the non-bend (YZ) plane need be only fine enough to assure that the muon came from the interaction point. Of course the rapidity measurement is of interest but for our purposes it is not crucial. So we will use only a crude charge-division position determination in the non-bend plane. The total number of wires, allowing for offset pairs to resolve the left/right ambiguity, is 360.

Backgrounds

Introduction

The apparatus is triggered by the scintillator telescope signals in coincidence with a beam-beam interaction signal. The minimum muon energy for the down arm telescope (SD1•SD2) is 2.1 GeV while for the up telescope (SU1·SU2·SU3) the minimum muon energy is 3.6 GeV. The beam-beam interaction signal will either come from some other experiment or be produced from forward/backward scintillator arrays installed by this group. Background events due to beam-gas interactions will be removed using timing information from this beam-beam signal. The remaining background events fall into two categories: those due to cosmic rays and those which are beam related. The momentum spectra of beam-produced events is relatively soft, and can be tolerated.

The cosmic background is considerably larger than the beam-associated background and requires the aboveground scintillator array for elimination. Cosmic muon events in the up arm can be cleanly removed in data analysis by the up-down time difference between SU3 and SU2 (40 ns). The down arm is more vulnerable to cosmic muons since timing cannot be used. Removal of cosmic muon events in the down arm will depend on track reconstruction. By reading out

both ends of SU3 and SU2 we can match the incoming cosmic track to the triggering track in the drift chambers. This SU2·SU3 umbrella allows us to reduce cosmic ray events to a negligible level offline.

The beam-beam produced background events occur at rates low compared to cosmic ray events. However, in this case no protection exists and the contamination is more serious. To estimate the two major backgrounds (π decay and punchthrough) we have used the CDF predictions[11] for π production. This facilitates comparison since the CDF model[6] has also been used for Drell-Yan and $W^{\pm}$ production (e.g., smearing of Jacobian peak ± 0.08). Our background and signal rates for μ^{+} are shown in Fig. 6.

Recall that this experiment has the minimum decay path and the maximum absorber possible in D0. Even so the backgrounds are substantial and more free path or less absorber could swamp the signal. It is basically for these reasons that we have chosen a closed geometry, especially since the Jacobian peak may well be less prominent than indicated in Fig. 6.

A summary of estimated background rates is given in Table I.

Cosmic Ray Background

Accidental coincidences with cosmic muons contribute the bulk of the trigger rate. This rate is estimated by first finding the number of counts in time T in a detector of area A which is placed in a flux of particles having a zenith angular distribution $dn/d\Omega = I_o \cos^j\theta$. If the detector has acceptance out to θ_{max} it sees N particles, given by

$$N = \frac{2\pi I_o A T}{j+2}\left(1 - \cos^{j+2}\theta_{max}\right)$$

where I_o is the vertical flux, integrated over energies greater than some minimum. For cosmic muons $j \sim 2$. For muons penetrating to SU1 (Item 1 in Table I) the minimum energy is 2.5 GeV and the integrated flux is 4.4×10^{-3} $cm^{-2}str^{-1}sec^{-1}$ [12]. In the calculation we use $\theta_{max} = 45^o$ and A = 100 ft^2. For accidentals involving muons counting only in the upper deck (items 5 and 8), $\theta_{max} = 90^o$, A = 225 ft^2, and the minimum energy is about 1 GeV. The number of cosmic rays in Table I has been increased by 25% over the results obtained for the up arm alone. This is to account for cosmic muons traversing the down arm but not the up arm.

To reduce this rate offline we will use somewhat different strategies depending on whether the cosmic muon triggers an up-arm event or a down-arm event. For up-arm events the relative timing of SU3 to SU2 establishes whether the muon was coming into or going away from the D0 area. For cosmic muons that trigger down-arm events we use the

end-to-end timing localization of SU2 and SU3 to remove tracks not going through the interaction point as determined by the innermost planes of tracking chambers. This reduces the solid angle factor such that roughly 400 triggers due to cosmic rays remain. Tight tracking constraints in the drift chambers are then used to reduce these to a negligible level.

Pion Decay and Punchthrough

To calculate the contribution of pion decay and punchthrough we need to estimate the absolute energy spectrum of produced pions. For most purposes we use the CDF model[11] which predicts the π° spectrum for $P > 15$ GeV/c. To calculate the number of background triggers however, we need to estimate the pion spectrum at much lower momentum ($P_{\pi} \geq 2$ GeV/c) as the great bulk of pion decay and punchthrough triggers will come from the spectrum near the cutoff energy. For this purpose we use a fit to 90° pion production[13] at $s = 52$ GeV given by

$$E\, d^3\sigma/dp^3 = 1.44 \times 10^{-26}\, p_T^{-8.6}\, e^{-11.9 x_T}$$

where we have doubled the coefficient to account for both charges. This gives 1.1×10^8 pions with $P > 2.1$ GeV/c pointing into our apparatus.

The pion decay probability in the iron is taken to be

$$P = 1.8\lambda_{INT}/\gamma c\tau$$

where the factor 1.8 accounts for multiplicity in pion interactions. λ_{int} is taken as 17 cm. We note the extreme sensitivity of the results to the cutoff momentum. This is mainly a reflection of the produced pion spectrum.

The hadronic punchthrough probability is estimated from a formula obtained by R. Kellogg[14] from both data and Monte Carlo simulations. For a pion incident on an iron slab the punchthrough probability is

$$P = \phi(P)\, e^{\frac{1000-X}{X_0}}$$

in which P is the pion momentum in GeV/c, X the absorber thickness in mm, and

$$X_0 = 185\text{mm} + 2.92(P-3.0)$$

$$\phi(P) = 0.0177\,(P-2.60) + 0.00168\,(5-P)^2 \quad 1.3<P<5$$

$$= 0.0177\,(P-2.60) \quad P>5$$

Although beam-produced pions create the second largest number of triggers, the momentum spectrum is rather soft. The rates are shown in Fig. 6, together with an indication of what is expected from W decays to muons. It is clear that the extra ranging in the up arm has a significant effect on the punchthrough background. We expect that the punchthrough signal in the down arm can be reduced at least

an order of magnitude offline. The drift chambers are read out at both ends for the charge division Z-coordinate determination. These measurements allow us to veto punchthrough events where the shower was sampled in any of the wire chambers. The punchthrough probability formula described above gives the total probability for any particle to exit after some depth. The vast majority of punchthrough events will have hadronic showers visible in the tracking chambers. Exactly what fraction will be removable is difficult to calculate but undoubtedly large. We also will have each scintillator half-plane summed signal in an ADC channel to provide independent shower sampling from the scintillator.

Alternative Configurations

The experiment has been designed to fit into the proposed D0 detector hall. We realize that the final hall may differ considerably from the present conception. Our apparatus can be modified to fit in anywhere - in particular we could mount an effective up spectrometer in the existing D0 tunnel without any detector hall at all. The apparatus as designed could also be rotated to horizontal from vertical, with $E_{\mu min}$ established by liquid scintillator tanks inserted into trenches on both sides of the berm. In general, the more magnetized steel the better, and the higher $E_{\mu min}$ the better.

Table I

Assumptions

Calendar time 300 hours. Luminosity $10^{30}cm^{-2}sec^{-1}$. Interaction cross-section 50 mb. A bunch crossing every 6 μs. Fast trigger coincidence resolving time 30 ns. Drift chamber memory time 1 μs. Offline coincidence resolving time 2 ns. E_μ(down) > 2.1 GeV. E_μ(up) > 3.6 GeV.

Process	Triggers	Comments
1) Cosmic muon in random coincidence with beam-beam interaction	1.1×10^6 up + down	Can be removed offline
2) Pion decay in 3" beam pipe	29K down 920 up	See Fig. 6
3) Pion decay in iron	135K down 2.2K up	"
4) Pion punch-through	5.2K down 515 up	"
5) Cosmic muon in larger iron detector in random coincidence with a pion decay	1450	Can be removed offline
6) Cosmic muon in larger iron detector in random coincidence with real muon (a spurious track)	10^{-3} extra tracks per event	"
7) Early cosmic muon in SU3 in accidental coincidence with real muon (incorrect rejection)	Probability per event = 3.9×10^{-4}	
8) Multiple muons due to extensive air showers in coincidence with beam-beam interactions		Excluded by real-time shower veto

References

1. Design Report for the Fermilab Collider Detector Facility (CDF) August, 1981

2. G.L. Kane, N.M. Gelfand Physics Opportunities for the Fixed-Target Tevatron, pg. 72.

3. Design Report, Tevatron Phase I Project, February 1980, Fig. 3 pg. 8 and Fig. 4 pg. 14

4. V. Barger et al., Phys.Rev.Lett. 42 , 1585 (1979) R.E. Schrock et al., Phys.Rev.Lett. 42 , 1589 (1979)

5. R.Lipton, Lepton Triggers for Heavy Quarks, pg. 109 of Reference 2.

6. Dechantsreiter et al., University of Wisconsin preprint DOE-ER-00881-202 (1981) See also Fig. 10.1 of Reference 1.

7. F. Paige, BNL-27066, Updated Estimates of W Production in PP and $\bar{P}P$ Interactions

8. See Fig. 1.2 and Table 1.1 of Reference 1.

9. C. Quigg, Rev.Mod.Phys. 49 (1979) 294

10. J. Owens, Jet Physics at Tevatron II, from Reference 2, pg. 169.

11. I. Hinchliffe and R.L. Kelly, Photon and π^0 Production at the FNAL $\bar{P}P$ Collider (CDF-83) See also Fig. 1.17 of Reference 1.

12. O.C. Allkofer et al., Phys.Lett. 36B, 425, (1971).

13. F.W. Busser et al., Nucl.Phys. B106 (1976) pg. 1.

14. R. Kellogg (U. of Maryland, Unpublished) These formulae incorporate data from F. Harris et al., NIM 103, 345 (1972), and calculations by T.A. Gabriel and B.L. Bishop, ORNL/TM-6132, and A. Grant, NIM 131, 167 (1975).

Figure Captions

1. Expected heavy flavor events as a function of $\sqrt{s}$ for an integrated luminosity of 10^{36} cm^2. For all but the $\bar{T}T$ events the daughter muons will be below the P_t cutoff of the apparatus. The daughter P_t spectrum folds the parent production P_t in with the semileptonic decay P_t.

2. Expected events from muonic decay of massive gauge bosons as a function of $\sqrt{s}$ for an integrated luminosity of 10^{36} cm^2.

3. Rapidity HWHM range for heavy particle production as a function of $\sqrt{s}$. The operating region of this apparatus is shown hatched.

4. End view schematic of the experiment in operating position at D0. The three up and two down scintillator planes are shown. The cosmic ray umbrella is formed from SU2·SU3. Tracking chambers and magnetic flux returns are not shown.

5. Detailed views of the lower spectrometer. The upper spectrometer is identical except for having a higher $E_{\mu min}$ due to the aboveground counters. The acceptance in θ is a function of where in the interaction region ($\Delta Z \sim 1.3$m) the interaction takes place.

6. Single μ^+ yield as a function of P_t for an integrated luminosity of 10^{36} cm^2. Sources include the massive gauge bosons, the Drell-Yan continuum, and background from pion decay and punchthrough. The total punchthrough background is the sum of that shown for the up arm plus that shown for the down arm.

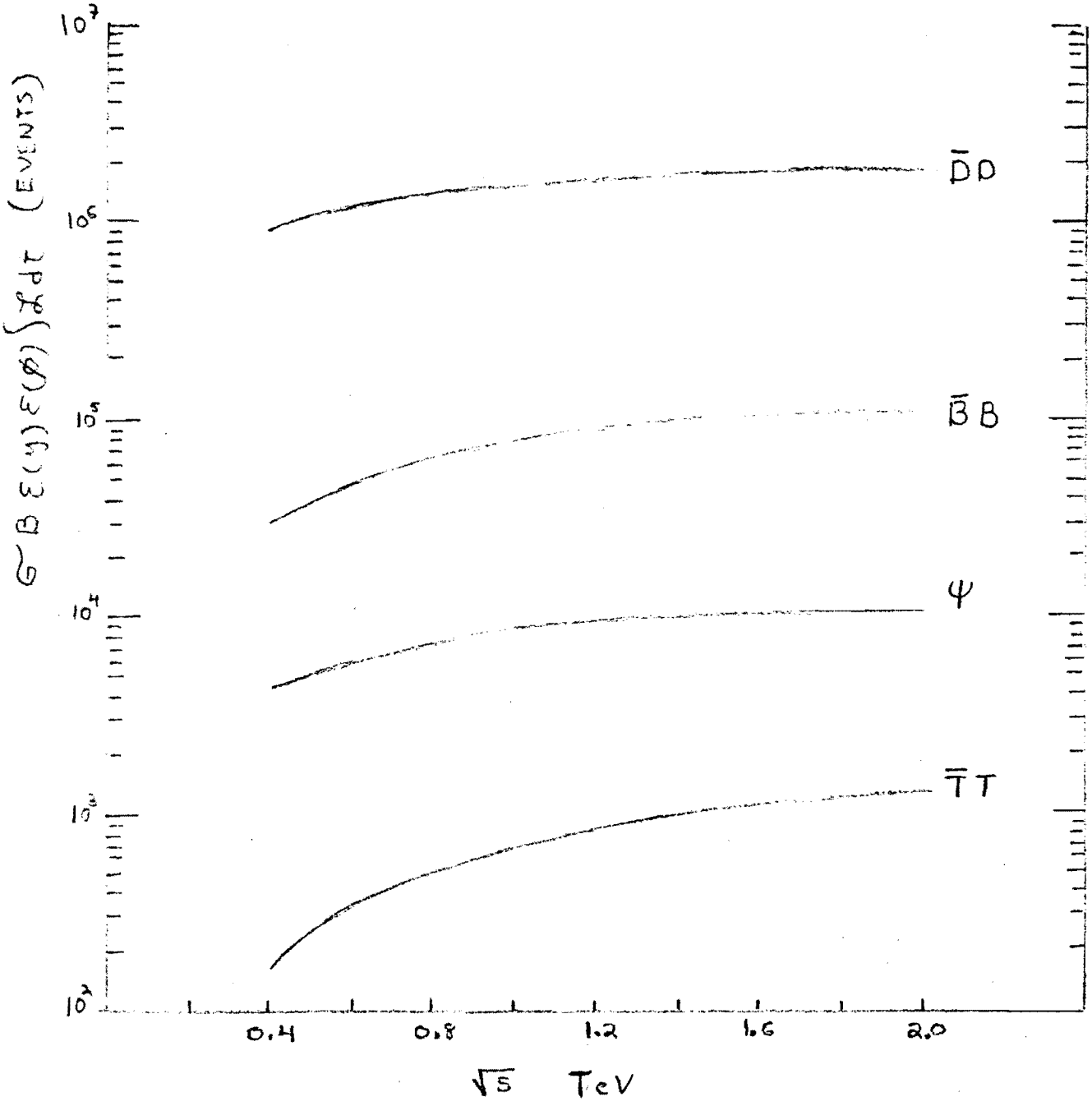
$\sigma_B \varepsilon(y) \varepsilon(\phi) \int \mathcal{L} dt$ (EVENTS)
10^7
10^6
10^5
10^4
10^3
10^2
$\bar{D}D$
$\bar{B}B$
ψ
$\bar{T}T$
0.4
0.8
1.2
1.6
2.0
$\sqrt{s}$ TeV

FIG. 1

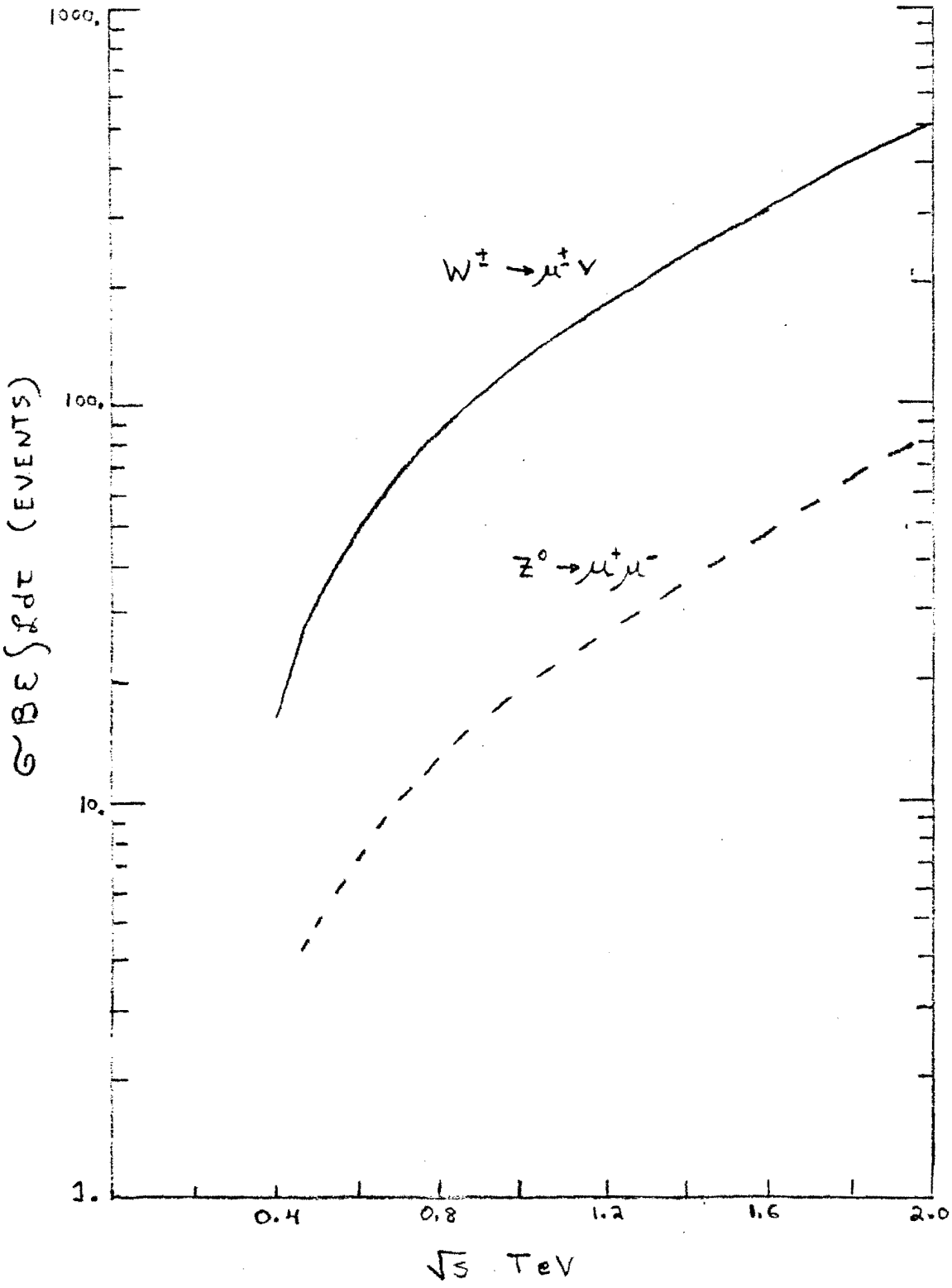
1000.
100.
10.
1.
$\sigma B \varepsilon \int \mathcal{L} dt$ (EVENTS)
$W^{\pm} \to \mu^{\pm} \nu$
$Z^0 \to \mu^+ \mu^-$
0.4
0.8
1.2
1.6
2.0
$\sqrt{s}$ TeV

FIG. 2

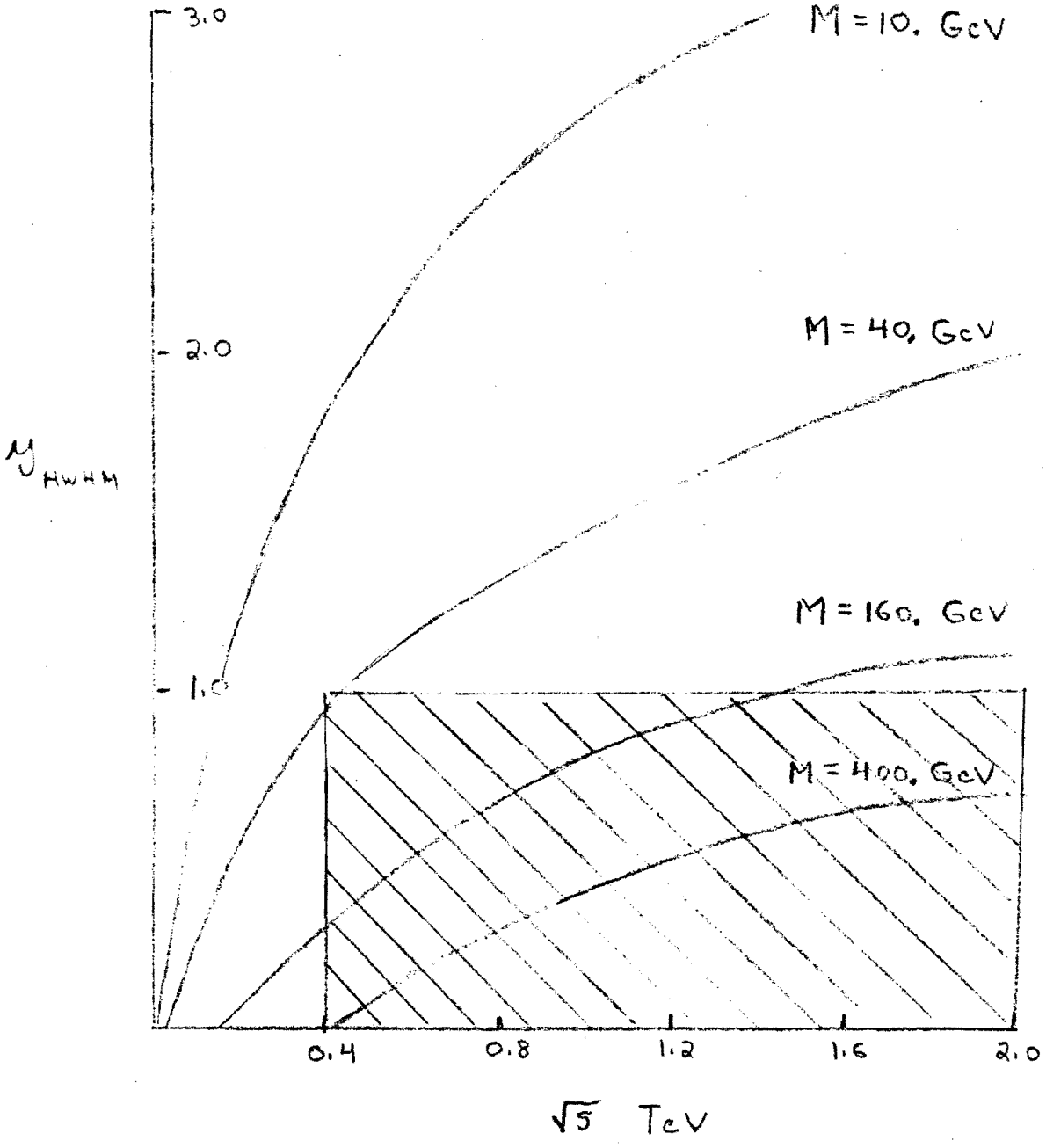
3.0
2.0
1.0
y_{HWHM}
M = 10. GeV
M = 40. GeV
M = 160. GeV
M = 400. GeV
0.4
0.8
1.2
1.6
2.0
$\sqrt{s}$ TeV

FIG. 3

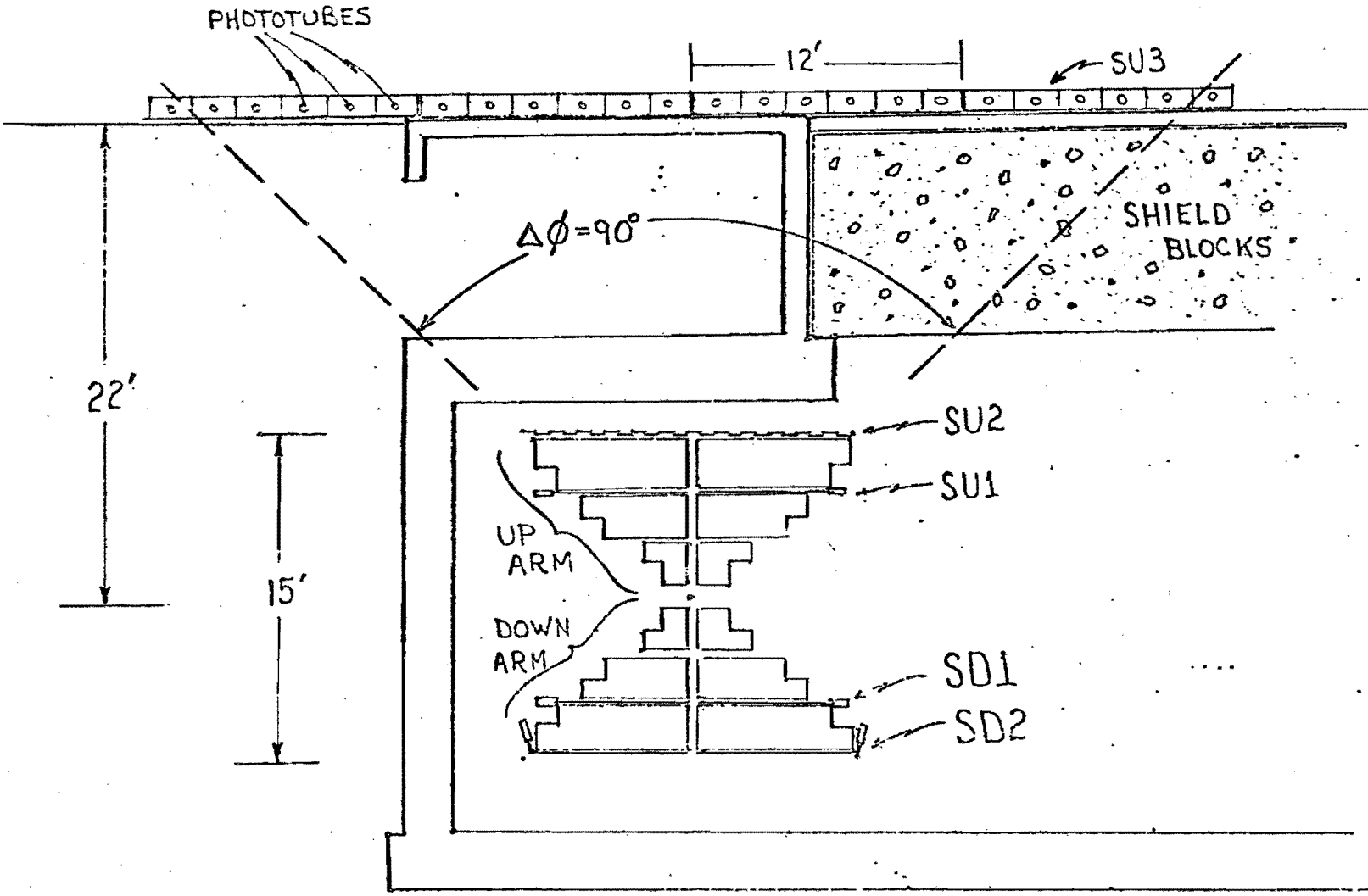
PHOTOTUBES
12'
SU3
SHIELD BLOCKS
Δφ=90°
22'
15'
SU2
SU1
UP ARM
DOWN ARM
SD1
SD2

FIG. 4

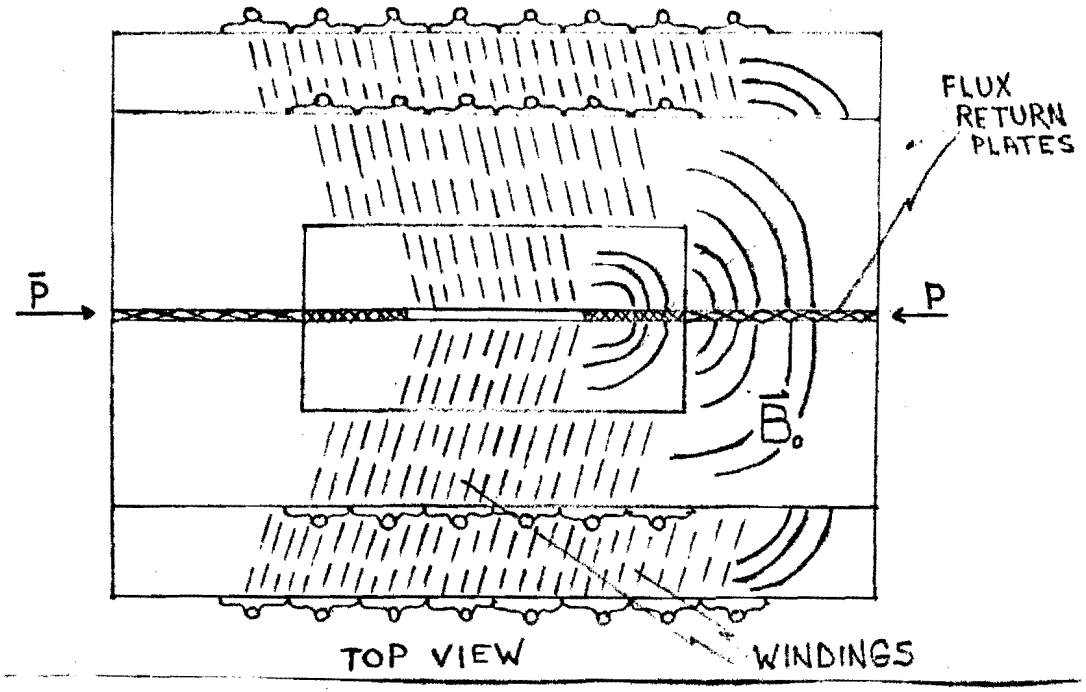

TOP VIEW

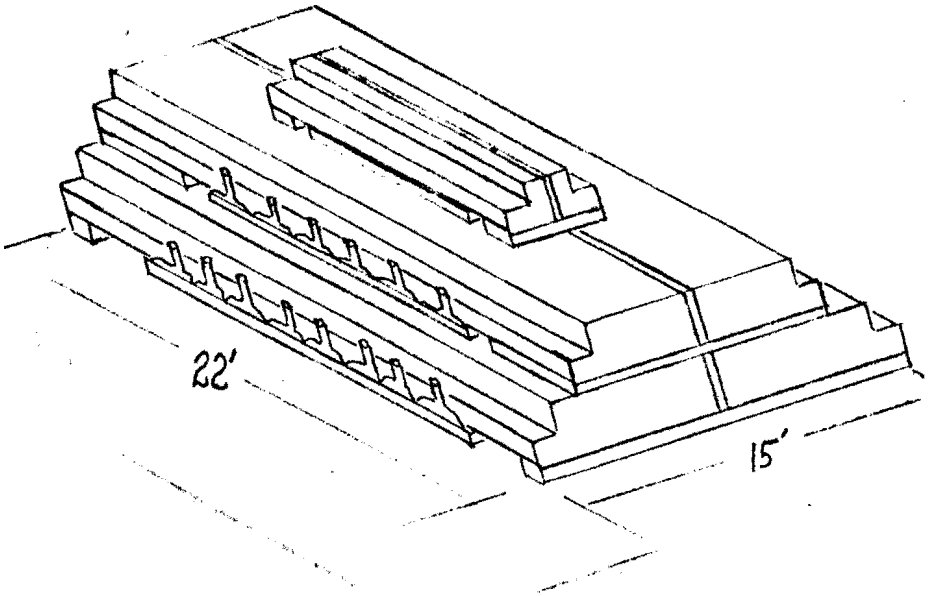

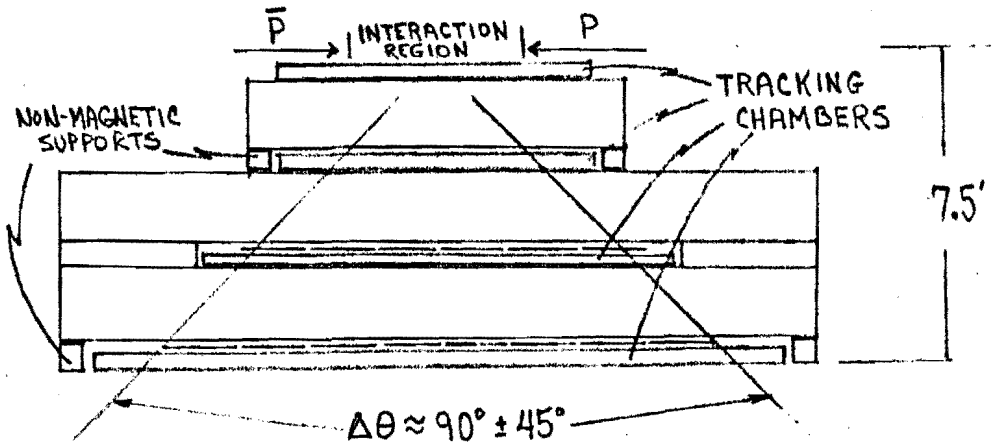

SIDE VIEW

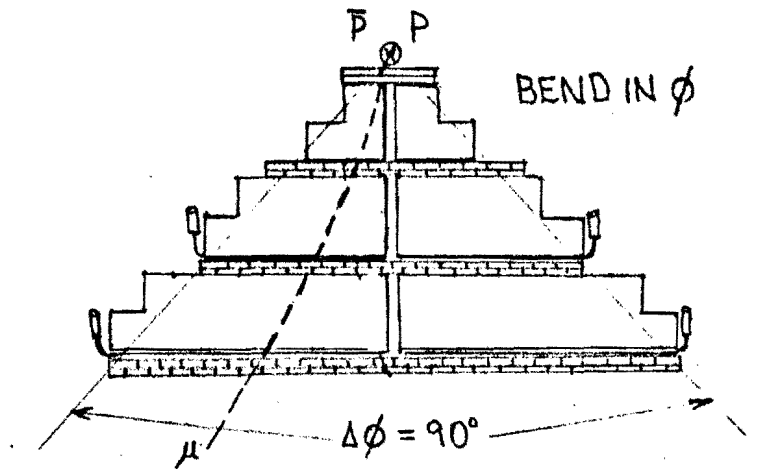

END VIEW

FIG. 5

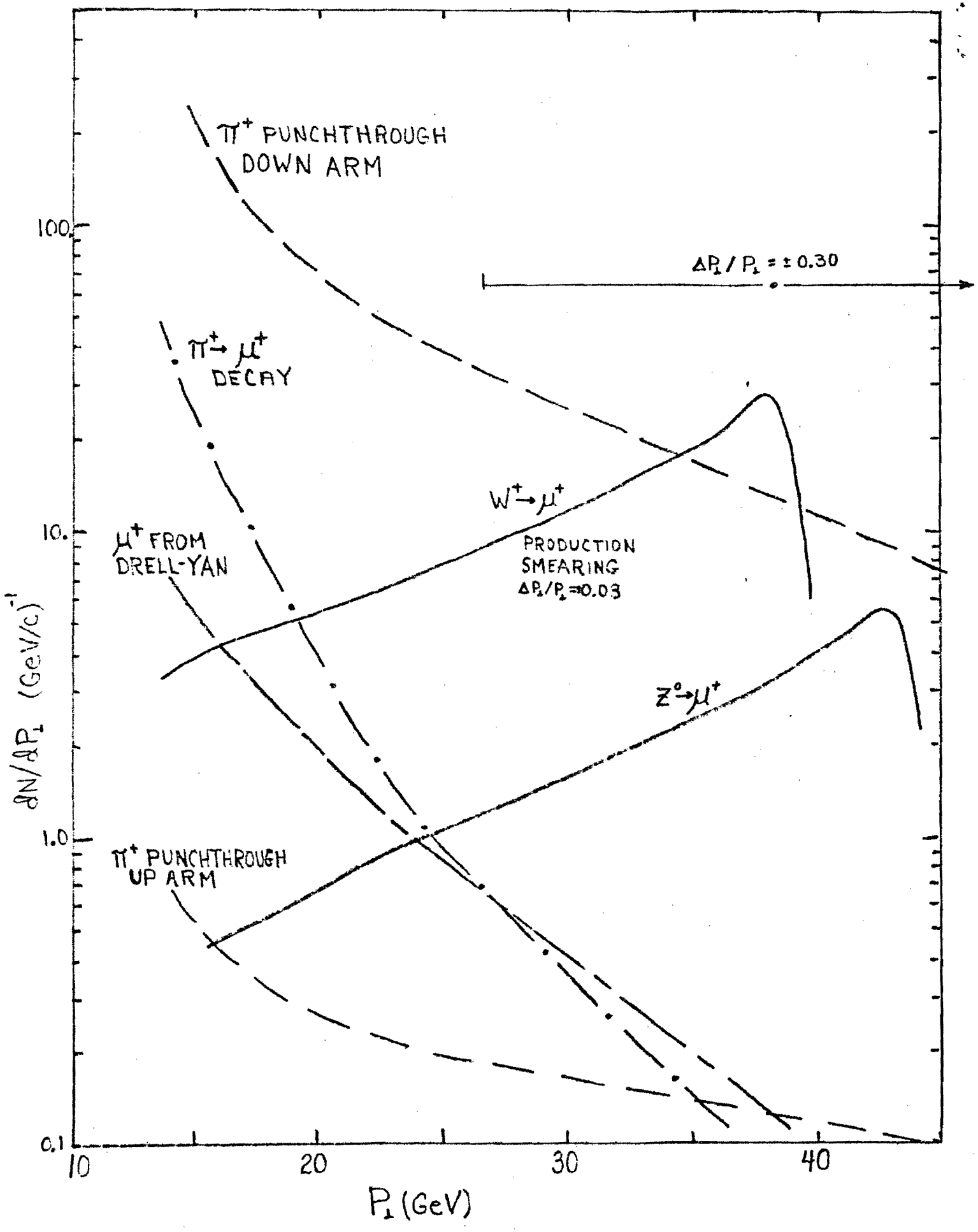
π⁺ PUNCHTHROUGH
DOWN ARM
ΔP⊥ / P⊥ = ± 0.30
π⁺→ μ⁺
DECAY
W⁺→μ⁺
μ⁺ FROM
DRELL-YAN
PRODUCTION
SMEARING
ΔP⊥/P⊥=0.03
Z°→μ⁺
π⁺ PUNCHTHROUGH
UP ARM
100.
10.
1.0
0.1
dN/dP⊥ (GeV/c)⁻¹
10
20
30
40
P⊥ (GeV)

FIG. 6

5/10/82

Fermilab Proposal No. P-712

Spokesperson: P. Rapp

Phone: (312) 840-4107

FTS 370-4107

STUDY OF MUONS FROM $\bar{P}P$ COLLISIONS UP TO $\sqrt{s}$ = 2 TeV

I. Revisions to the original proposal (2/1/82).

II. Response to the PAC concerns (4/6/82).

May 18, 1982

Abstract We propose to measure the production of muons from the FNAL collider as a function of $\sqrt{s}$ and p_t. At low luminosity we can use the varying absorber length to separate and measure pion and prompt muon production. This beam dump mode allows us to measure the backgrounds leading into the electroweak boson region, a feature not available to either CDF or P-714 ("LAPDOG"). Our detector measures like-sign dimuons, a powerful handle on backgrounds unavailable to LAPDOG. Most important, our background from punch-through and pi-decay is a factor 15 below that for CDF, allowing any muon signal to be that much more cleanly seen. This will be especially important if the pion background is larger than expected or if the production of heavy masses is more momentum-smeared than expected. Total cost of the experiment, including low-beta quads and construction of the D0 area, is less than 10% of the cost estimated for CDF.

This letter contains two parts:

I Changes since P-712 was submitted

II Response to the PAC concerns (letter of 4-6-82.)

In section II we concentrate especially on demonstrating the unique physics capabilities of our apparatus relative to CDF.

I Changes and impact of changes

(a) Additional Collaborators. The collaboration has been broadened to include more University participation. The list now includes:

University of Arizona: Burt Pifer

George Mason University: Bob Ellsworth

University of Maryland: Pat Rapp (Spokesperson)

Virginia Tech: John Ficenec

Fermilab: D. Green, H. Haggerty, E. Malamud

(b) Increased acceptance. We have dropped the idea of trying to share the large angle region with another group. Both experiments in such an arrangement are compromised and a better solution is to run them in different years. Better physics is done by enlarging our apparatus to cover, for large polar angles, full 2-pi azimuth. The revised geometry is shown in Figure 1a,b,c.

(c) Field direction. As seen in Fig. 1 the field direction is now rotated 90° from our original proposal. Although we could still design a magnet with the original orientation, once we go to 2-pi geometry a toroidal magnet has a particularly simple mechanical solution.

(d) Weight. The steel is now increased from 530 tons to 964 tons. In this new geometry all the steel is efficiently used for momentum analysis and ranging. At the core of the detector, inside the radius of the main ring, is 15 tons of copper (Fig. 1). This copper core is an efficient non-magnetic pion absorber and thus minimizes the magnetic field gradient across the main ring. We can do even better if tungsten or heavimet can be obtained.

(e) Triggering. The aboveground liquid scintillators are eliminated, leaving the detector completely underground and with left/right/up/down symmetry. p_{min} is kept large by substituting the central copper for the external dirt. Cosmic ray triggering is minimized by dividing the non-bend projection into 32 triple-coincidence triggers. (Fig. 2) Each trigger telescope points at the beam line. Off-line, cosmic events are removed using the full-azimuth tracking. Up-down timing from the outermost scintillator counters is used also to reject cosmic background to the dimuon spectrum.

(f) Tracking. There are now three tracking stations, each covering full 2-pi azimuth. (Fig. 1) Each station has 10 layers of drift tubes (Fig. 3) and yields a track vector accurate to $\pm$ 1mr. These three vectors yield essentially two independent measurements of the momentum. They also

provide a very tight 'Coulomb telescope' on a multiply-scattering muon, serving to distinguish the muon from candidate trajectories derived from a particle cascade.

(g) Magnet power. The magnets are excited to 15 kg with 140 turns and 100 amps. Power is 10 kw. Water cooling is not needed. The magnets will not be driven into saturation, since fringe field at the main ring beam location is critical.

(h) Stray field problem. Both the Main Ring and Doubler beam pipes pass through field free regions. Since the steel is not saturated we do not anticipate difficulty in shielding these pipes. We think the magnet can be on while the Main Ring is running. But, of course, we have to convince ourselves and the Accelerator Division of this. A rough estimate of the unshielded field and field gradients in the region of the Main Ring pipe are a few gauss and a few tenths of a gauss/cm. We feel that these fields are small enough to shield. All steel plates will be machined so as to keep field leakage into air gaps at a minimum.

(i) Assembly and Testing. The low power requirement makes it easy to assemble the complete magnet in an industrial building and measure the stray fields in the region of the beams. This will also enable us to work out

and rehearse an efficient installation scenario.

(j) Installation. No caissons are needed. A "garage" for assembly is useful but not necessary if an overhead crane (capacity $\gtrsim$ 20 tons) is available. After assembly the region above our experiment would be plugged with concrete blocks and/or backfilled with dirt. A rough estimate, to be refined later, is that installation could be done in 20 working days (2 shifts/day).

(k) Size of area. Our apparatus is a cube 20' on a side. This cube gives us $\pm$ 45 ^{o} coverage in polar angle, 2-pi azimuthal coverage, and thickness on all sides of 12.6 absorption lengths, minimum. P_{min} is 2.5 Gev/c for muons at normal incidence to the copper and is larger for muons at slant incidence. We feel, as discussed in Section IIe that punch-through is potentially a severe enough problem that this thickness is necessary. Because the detector occupys only 20' along the beam, only a few beam elements need to be rearranged when converting back to fixed-target operation (D0 extraction). It is possible that removal of the central copper, leaving a space 40" x 40" centered on the Saver pipe, would allow fixed-target operation with the steel remaining in place for the next collider running.

(l) Costs. The total cost is estimated at $1150K, which breaks down into $700K for the magnet, $24K for the copper core, and $425K for the detectors and associated electronics (4160 drift cells, 2134 ft^2 of NE102 scintillator, 160 phototubes, 4320 ADC's, and 160 TDC's). We note that even at full price, and including $4M for the low-beta quads and the D0 area, the total cost is less than 10% of the $60M estimated for CDF.

II Response to Questions

(a) Unique Physics capabilities relative to CDF. Clearly both CDF and P-712 propose to study final state muons. The main thrust of P-712 is that CDF is designed around tracking and calorimetry and, as such, makes some compromises with muon physics. We assert that in two crucial aspects, pion and kaon decay to muons and hadronic punch-through, P-712 will do a superior job. As explained in detail below, we find that our background due to these sources is a factor 15 below that for CDF. (Fig. 5) The pion source spectrum used is the same used by CDF[1].

(b) Luminosity Requirements. Naturally, any experiment designed to study electroweak physics requires high luminosity. Thus eventually, like most other users in the D0 area we will request a low-beta insertion of reasonable strength, e.g. beta of 3 - 4 meters. Under initial low luminosity running conditions interesting physics can be extracted from P-712. For example, the mu $\pm$ yield due to heavy flavor production falls many orders of magnitude between our 2.5 GeV/c p_t cutoff and the electroweak regime ($p_t \sim 40$ GeV/c). This is shown in Fig. 4. The yield from pi-decays and punch-through displays similar behavior. By utilizing the varying path lengths through the detector, by making minor changes in the decay path, and by measuring same sign and opposite sign dimuons, we will be able to separately extract the yield of pi $\pm$ as a function of p_t, and the yield of prompt muons vs. p_t. In this respect P-712 is basically a beam dump experiment. This "moderate" p_t physics, $3 < p_t < 10$ GeV/c is interesting in itself and will serve as a prelude to electroweak physics. Note that the thin CDF detector necessitates a trigger p_t cutoff $\gtrsim 10$ GeV/c which precludes that CDF study this sort of physics.

(c) Solid angle acceptance. As already discussed we have increased the azimuthal coverage to 2-pi. This results in a W^+ efficiency of 50% and a Z^o efficiency of 33%. In rapidity we cover 2.0 units, compared to 2.2 for the central

detector of CDF.

(d) (1) Background from pi-decay. We believe that the problem of pion decays has been optimized in P-712. The relevant scale factor is the available decay path, equal to the distance in air plus one lambda of absorber. For our detector this number is 20 cm. In comparison, CDF uses a conservative figure of 180 cm for the total decay path. This means that P-712 is lower by a factor of 9 in pi-decays, equivalent to a factor of 2 in momentum. This factor may be crucial if the Jacobian peak is not as pronounced as indicated in the model used by the CDF group. The question of the Jacobian peak will be discussed below in Section IIf.

(d) (2) Background from heavy flavor decay. If the top quark has a mass of 20 GeV,then the expected background has a magnitude and shape rather like that indicated in Fig. 4 for pi-mu decay. Again, by using varying path lengths through the absorber, we can separate the prompt muon yield from the pi-decay yield.

We emphasize the fact that P-712 measures charge, and therefore can use like-sign dimuons to get a handle on background sources. This capability is, for example, not available to P-714 ("LAPDOG"). We assert that, using

like-sign dimuons, we can reduce the heavy flavor background, at least in a statistical and model dependent fashion, below that due to pi-decays. The like and unlike-sign dimuon background shapes with respect to the Drell-Yan and Z^{o} signal are shown in Fig. 5 as an example.

(e) Punch-through. We feel that a great strength of P-712 with respect to CDF is in the problem of hadronic punch-through. Basically CDF has a thin absorber, 6.4 lambda, while P-712 has a thick absorber, 12.6 lambda. This means that the probability per hadron to pass through the absorber without interacting is 500 times worse for CDF.

Because we do not sample the energy deposition of the muon as does CDF, we have a background from showering punch-through in addition to the background from non-showering punch-through. To remove this shower background we use the "Coulomb telescope" described in Ref. 2 (Fig. 7). We have conservatively estimated our rejection by taking the square root of Rubbia's rejection factors (F in Fig. 7b), assuming only a one-dimensional telescope in our non-bend plane. In reality we expect the rejection to be much better since on each candidate track we have three vectors which must yield trajectory uncertainties consistent with the multiple scattering of a muon having the calculated momentum. Monte Carlo studies are necessary to

determine accurate rejection factors. Our conservative estimation yields a showering punch-through signal equal to a few times the non-showering punch-through signal. In sum, our better rejection of the substantial punch-through background is one reason that P-712 is superior for doing muon physics.

Along this line we note that rejection by sampling kills any muon accompanied by a nearby showering particle. This may be risky.[2]

(f) Momentum Resolution The weakest point of P-712 is momentum resolution. Our stated momentum resolution of $\sigma/p = \pm 14\%$ is a compromise between our analytic calculation, confirmed by Monte Carlo, and the scaled results from Mark J and Ting's ISR dimuon experiment. Our calculation gives $\pm$ 12.8%, using a field of 15 kg and a spatial resolution of $\pm$ 200 microns.

Scaling by magnetic field strength and the square root of the path length we get $\pm$ 20.5% from Mark J, which sampled the track with vector, point, vector, and $\pm$ 16.7% from the ISR experiment, which sampled using 3 or 4 points and a vector. Our track sampling (vector, vector, vector) is shown by analytic calculation to be more accurate than either of these other methods. In essence we have two

independent momentum measurements. Scaling the two reported results by accuracy of track sampling gives resolutions around $\pm$ 15%. Using our calculation and the two scaled estimates we have settled on $\pm$ 14% as our present best estimate. The resultant smearing of the W peak is graphed in Fig. 8.

We feel that punch-through and decay are problems of sufficient gravity that we choose to compromise on momentum resolution. Using the CDF model of W production, P-712 can easily see the Jacobian Peak (with delta-$p_t/p_t = \pm 0.08$) because we have reduced the punch-through and decay backgrounds. For CDF the thin absorber far from the interaction implies a poor peak to background ratio (Fig. 9). We note that many QCD models have a more badly smeared peak due to gluon radiation. If this be true, then background rejection is much more important than momentum resolution. An example due to Paige[3] is indicated in Fig. 6.

We hope that this response adequately addresses the concerns expressed by the PAC. We would be very happy to discuss any of these points in more detail with any member of the PAC.

References

1.) I. Hinchliffe and R. L. Kelly, LBL-12274, CDF-83, Photon and Pi-zero Production at the FNAL Collider, February, 1981.
See also Design Report for the Fermilab Collider Detector Facility (CDF), August, 1981, Fig. 1.17.

2.) Proposal for a 4*pi Solid Angle Detector for the SPS Used as a $\bar{p}p$ Collider at a Centre of Mass Energy of 540 Gev, CERN/SPSC/78-06, SPSC/P92, January, 1978.

3.) F. Paige, BNL-30805, Monte Carlo Simulation of Heavy Quark Production in pp and $\bar{p}p$ Reactions, January, 1982.
See also F. Halzen, A. D. Martin, D. M. Scott, MAD/PH/41, DAMTP82/5, Does Large Transverse Hadronic Energy Accompany Drell-Yan Photons and Weak Bosons?, March, 1982.

Figure Captions

1. Three views of the revised detector. Note that the absorber length is a minimum of 18" Cu plus 64" Fe, a total of 12.6 lambda.

2. Schematic of the 32 triple-coincidence scintillator telescopes used to trigger on muons. The telescopes point to the interaction region (width approximately 2 mm.) in the non-bend plane. They are instrumental in lowering the cosmic ray triggering rate.

3. A cutaway of one of the 3 full-azimuth triggering and tracking stations shown in Fig. 1. Each station consists of overlapped triggering scintillator counters and 10 layers of drift cells. Each station provides a vector accurate to $\pm$ 1 mr. in either projection. The three vectors on each track give accurate momentum determination and constrain muon candidates to a tight "Coulomb telescope", allowing near-elimination of showering punch-through background.

4. An indication of how the detector can be used in a beam dump mode at low luminosity. The varying path length through the absorber allows separation and measurement of the pion and prompt muon spectra. Here the specific comparison is between top decay and pion decay. Determination of the background signals leading into the electroweak boson region is essential to understanding that region. Neither CDF nor LAPDOG can operate in the beam dump mode.

5. An estimate of the heavy quark background contribution to Drell-Yan production of dimuons. Also indicated is the need for like-sign dimuon measurement to understand the unlike-sign dimuon signal. LAPDOG cannot distinguish like-sign and unlike-sign pairs.

6. The background from pion decay and punch-through for this proposal and CDF. Both derive from the pion source spectrum of Ref. 1, also shown in the figure. The P-712 background is a factor 15 below the CDF background. Also shown is the muon signal from W^+ decay as estimated by CDF[1] and by Paige.[3]

7. The top figure is a schematic of the Coulomb telescope of Ref. 2, pp. 101-104. Fig. 7b gives rejection factors for showering punch-through mimicking a multiply-scattering muon. To estimate our rejection factors we have very conservatively used the square root of F indicated in the figure. See part II, section (e) for discussion.

8. The effect of our momentum resolution ($\sigma/p = \pm$ 14%) on the single muon signal from W^+.

9. A comparison of the single muon spectrum seen by this proposal and by CDF. The factor 15 reduction in pion decay and punch-through background gives this experiment a much purer sample of W events.

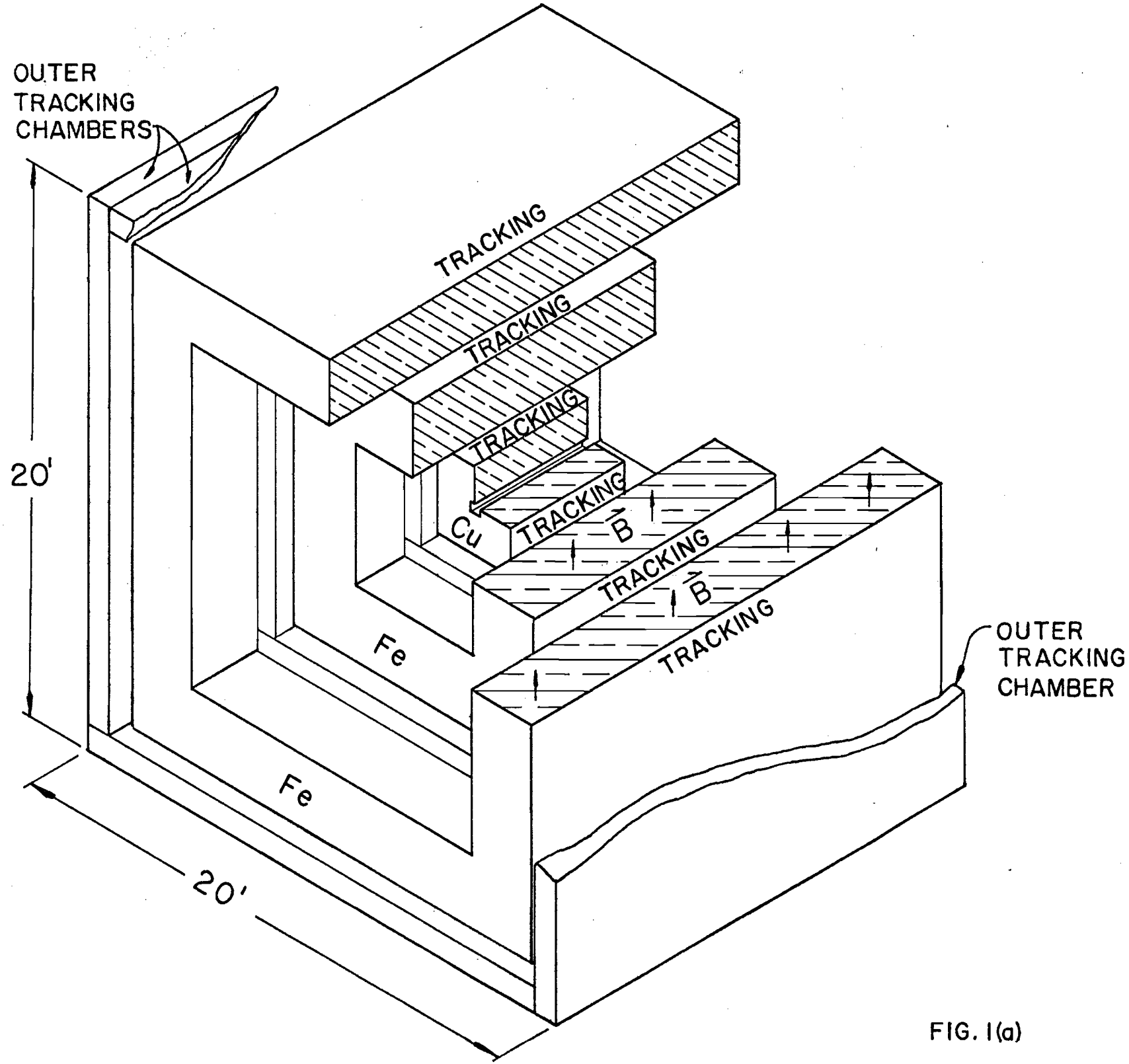
OUTER
TRACKING
CHAMBERS
TRACKING
TRACKING
TRACKING
TRACKING
TRACKING
TRACKING
20'
Cu
B
B
Fe
Fe
20'
OUTER
TRACKING
CHAMBER

FIG. 1(a)

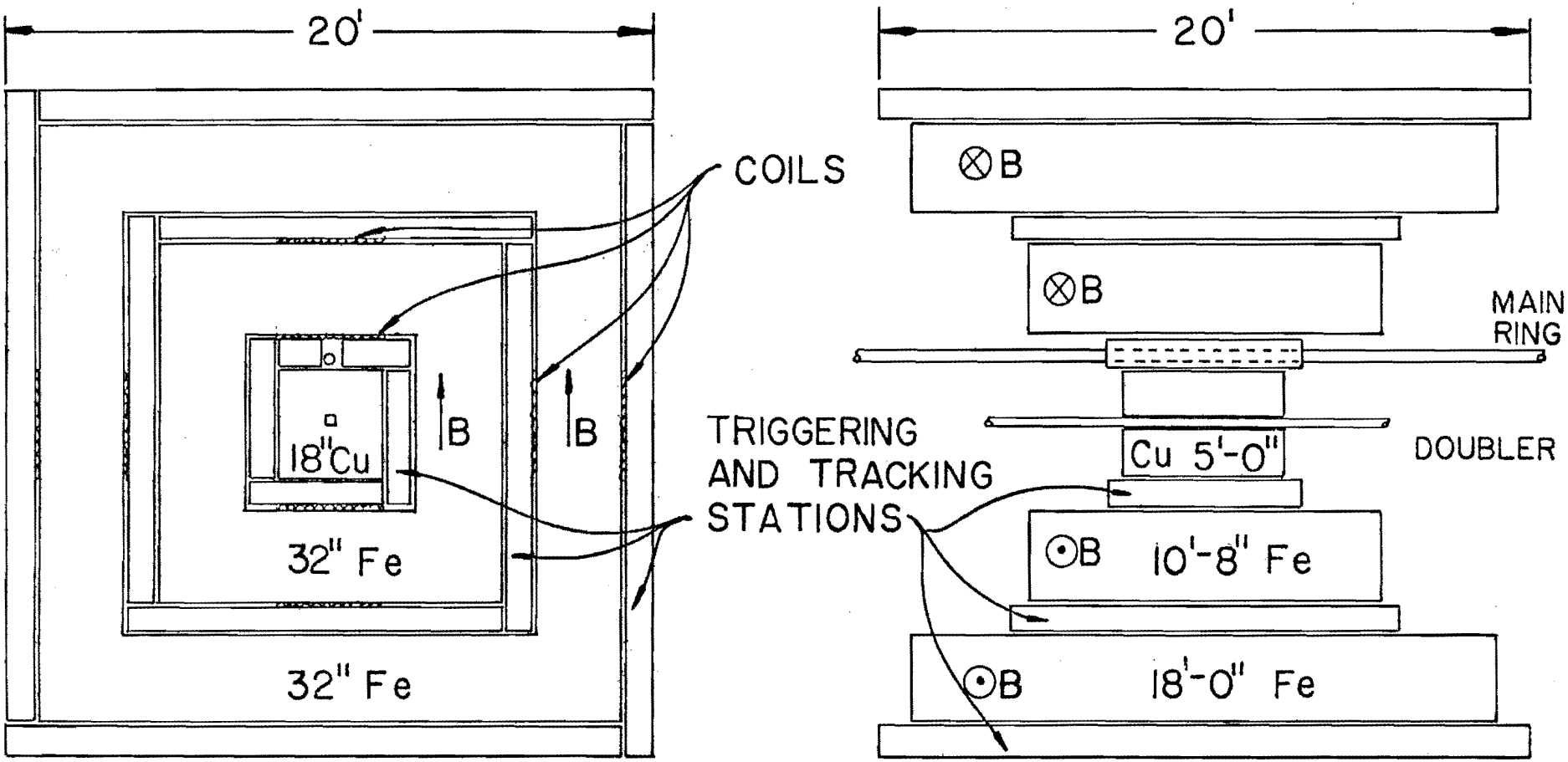

END VIEW

FIG. 1(b)

SIDE VIEW

FIG. 1(c)

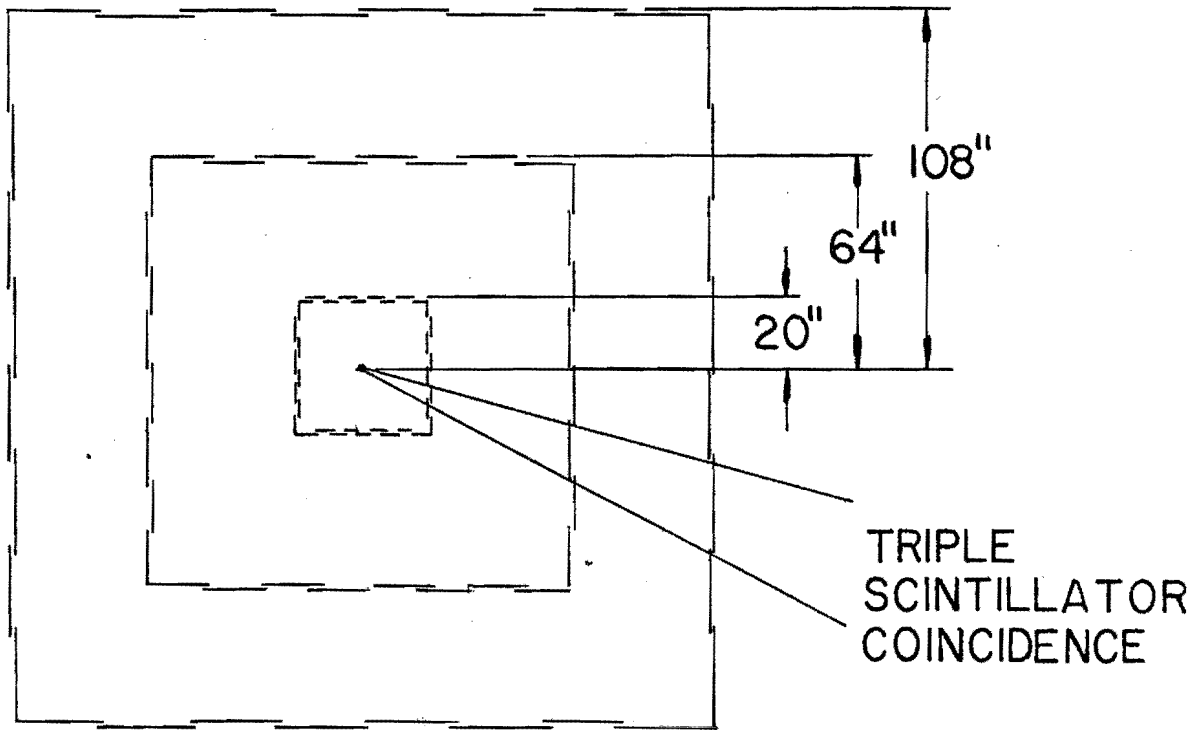

32 TRIGGER TELESCOPES

FIG. 2

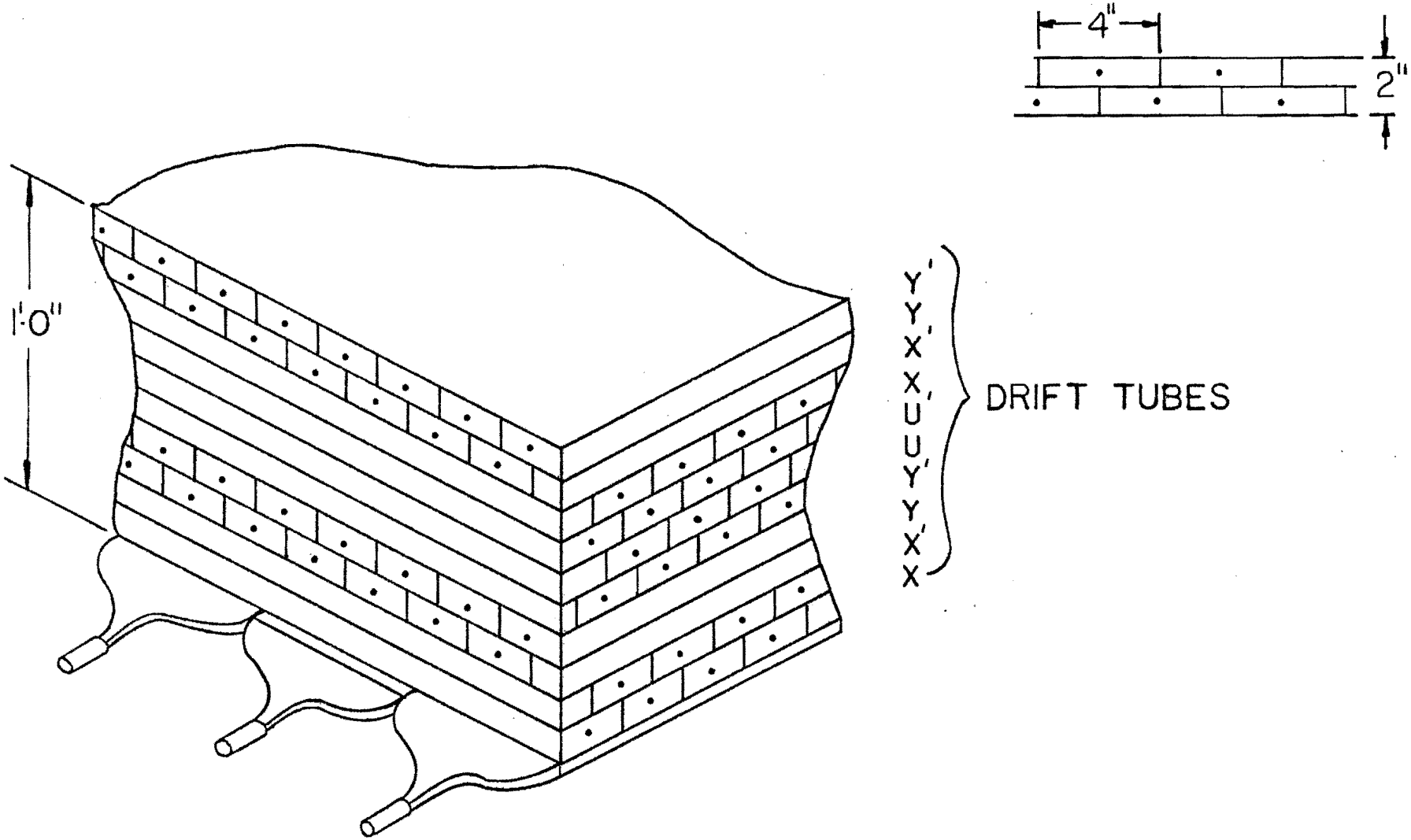

TRIGGERING AND TRACKING STATION

FIG 3

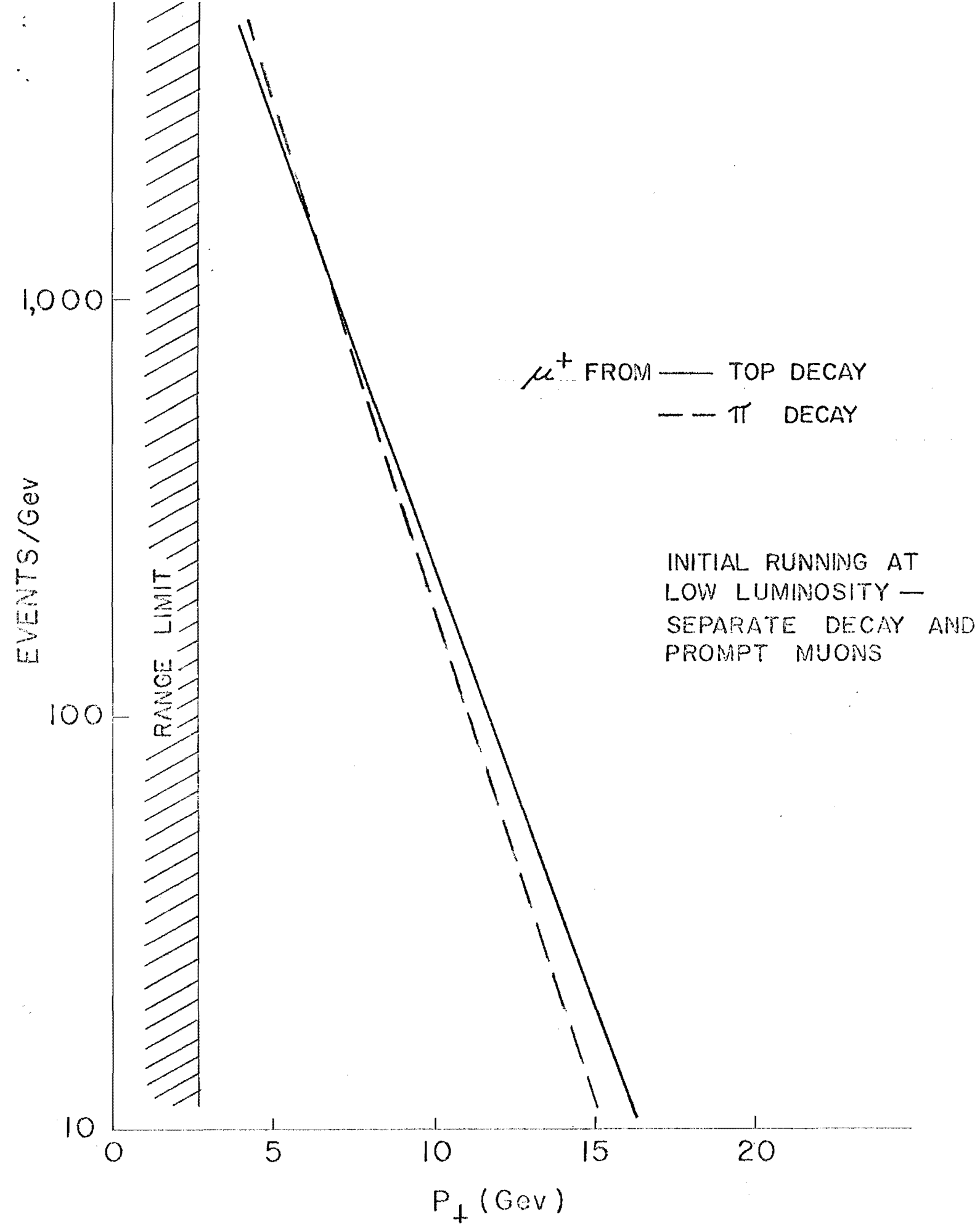
1,000
100
10
EVENTS/Gev
RANGE LIMIT
μ^+ FROM —— TOP DECAY
— — π DECAY
INITIAL RUNNING AT
LOW LUMINOSITY —
SEPARATE DECAY AND
PROMPT MUONS
0
5
10
15
20
P_+ (Gev)

FIG 4

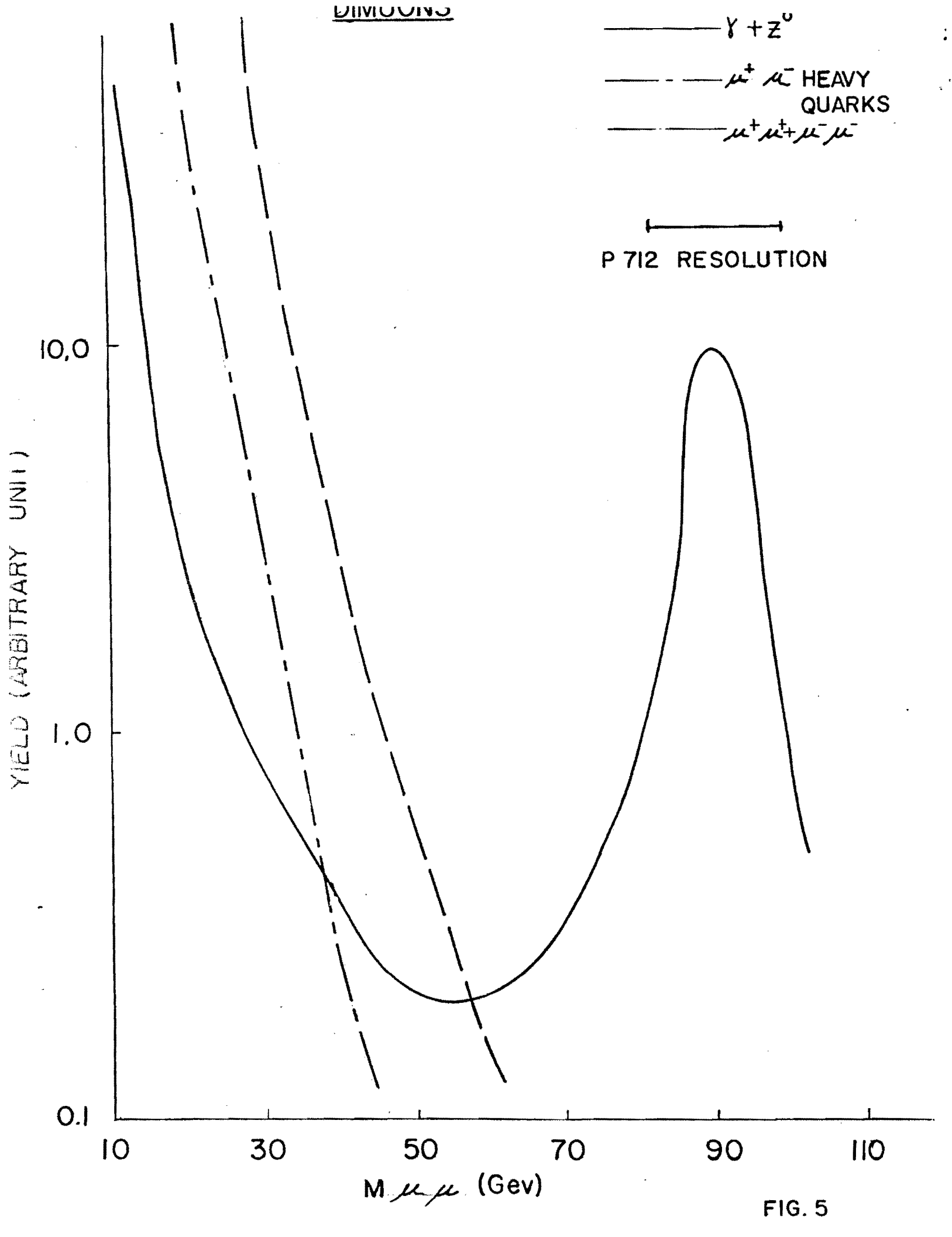
DIMUONS
$\gamma + Z^0$
$\mu^+\mu^-$ HEAVY QUARKS
$\mu^+\mu^+ + \mu^-\mu^-$
P 712 RESOLUTION
10,0
1.0
0.1
YIELD (ARBITRARY UNIT)
10
30
50
70
90
110
M $\mu\mu$ (Gev)

FIG. 5

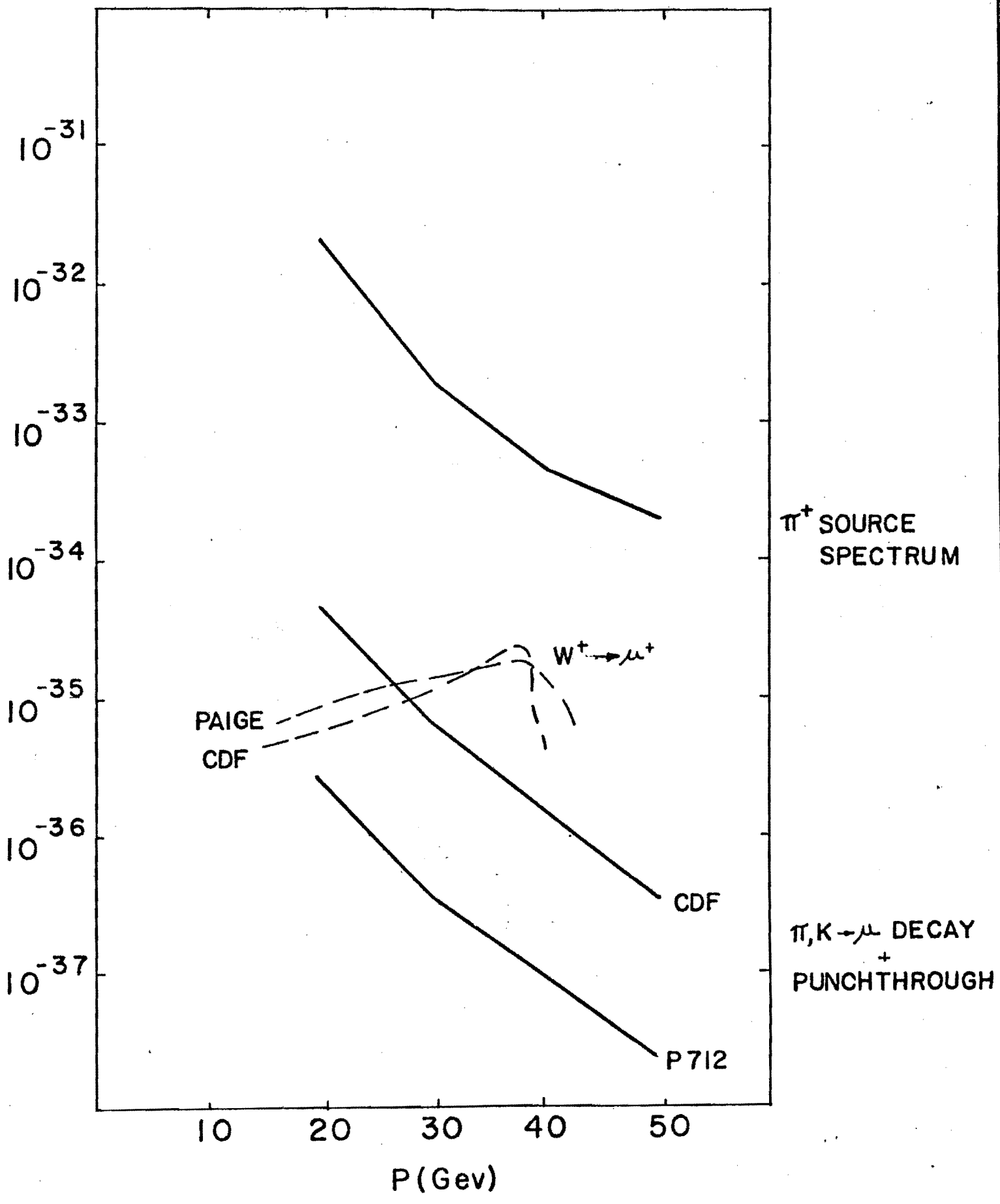
10^{-31}
10^{-32}
10^{-33}
10^{-34}
10^{-35}
10^{-36}
10^{-37}
$d\sigma/dp_t dy|_{y=0}$ cm² (GeV/c²)
10
20
30
40
50
P (Gev)
π^+ SOURCE SPECTRUM
$W^+ \rightarrow \mu^+$
PAIGE
CDF
CDF
$\pi, K \rightarrow \mu$ DECAY + PUNCHTHROUGH
P712

FIG. 6

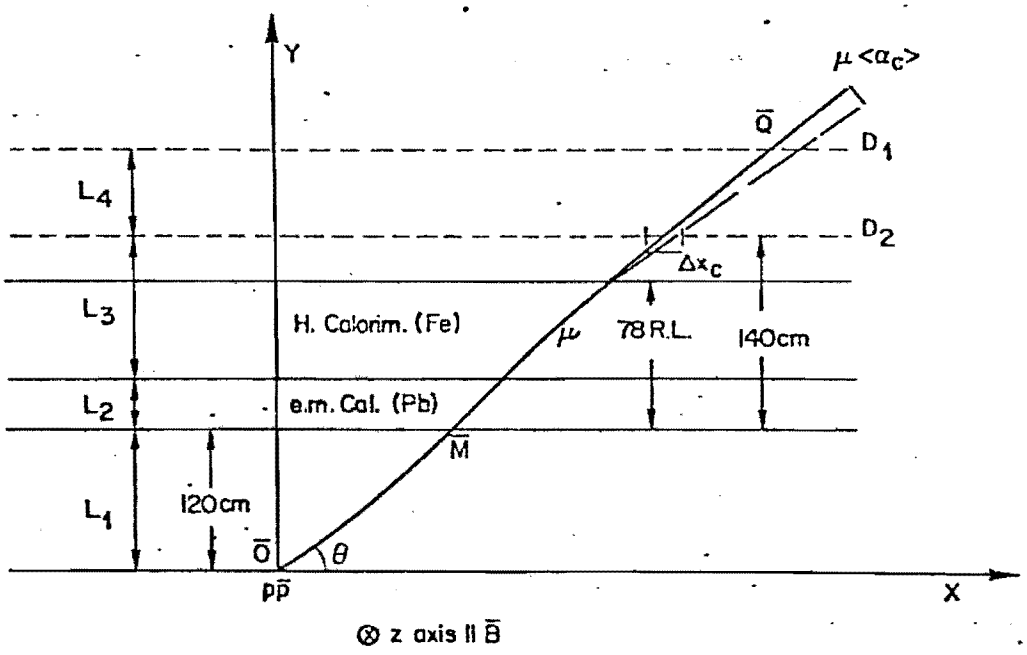

Figure 7(a) Schematic layout for study of the rejection function F(p). A muon traverses drift chambers D_1, D_2 with an indetermination Δx_c Δy_c due to errors reconstructing track $\overline{OM}$ and Coulomb displacement, and Coulomb scattering $\langle\alpha_c\rangle$. One pion emerging from a hadronic shower in iron has a much larger $\langle\alpha_H\rangle$ and Δx_H.

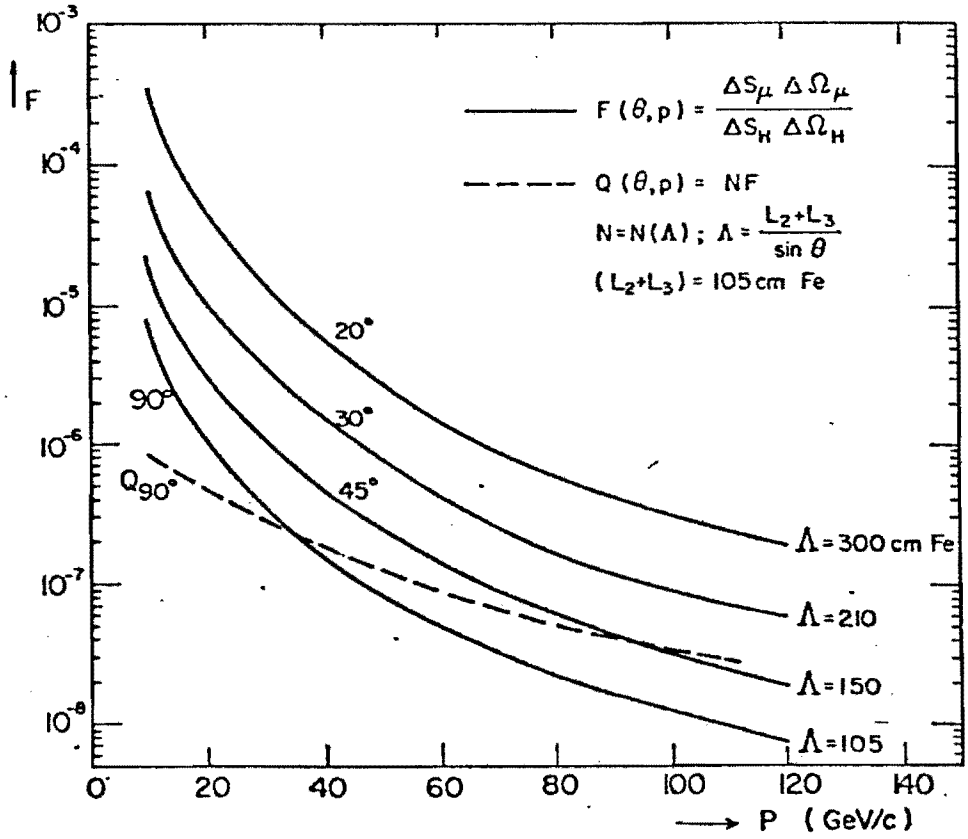

Figure 7(b) Function $F = (\Delta S_c/\Delta S_H)(\Delta\Omega_c/\Delta\Omega_H)$ probability of having a hadron within the "Coulomb telescope" of a muon. $Q = NF(p)$, total probability as above for N hadrons emerging from the iron in a very high energy event.

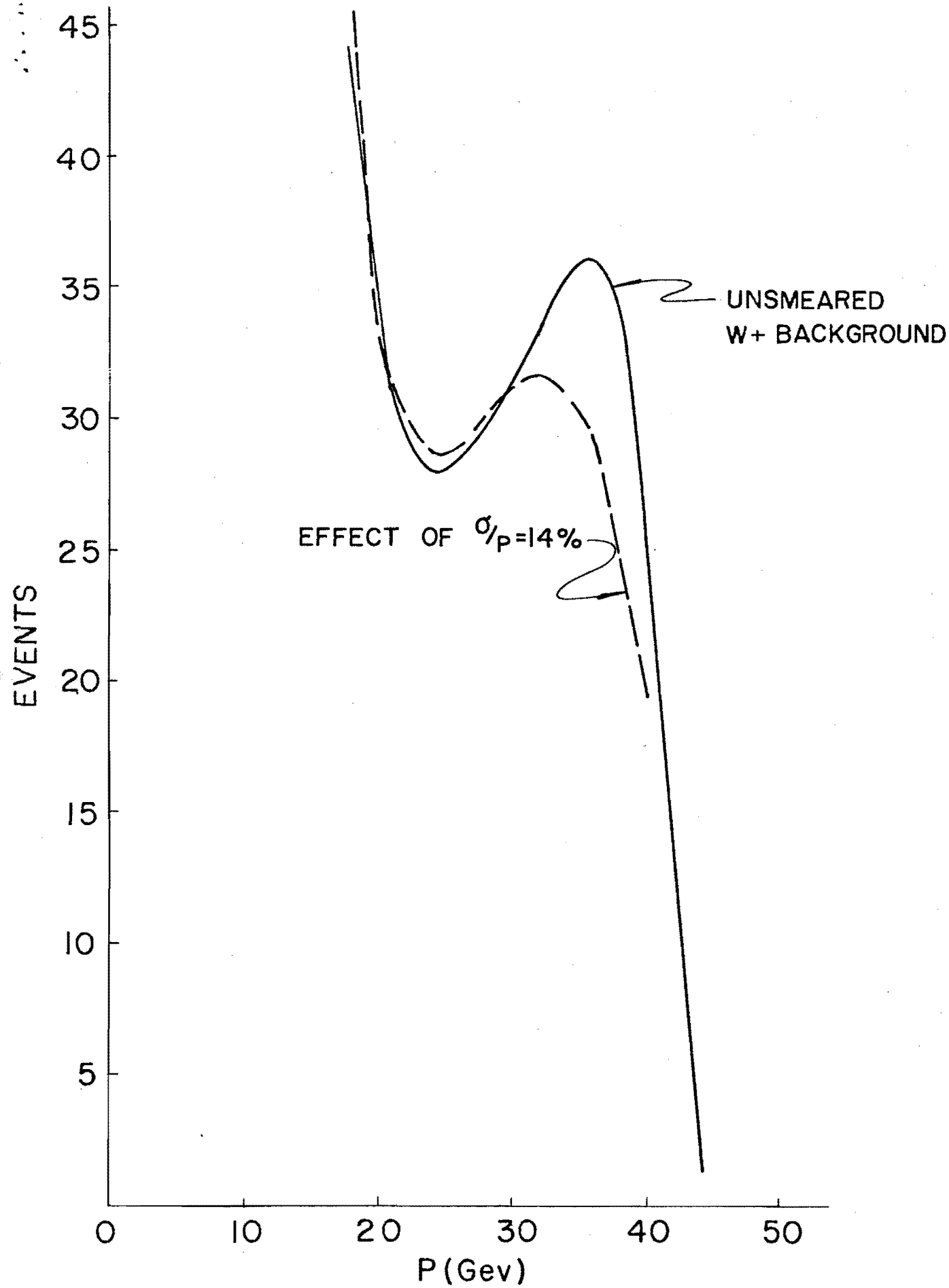

P 712 MOMENTUM SMEARING

FIG.8

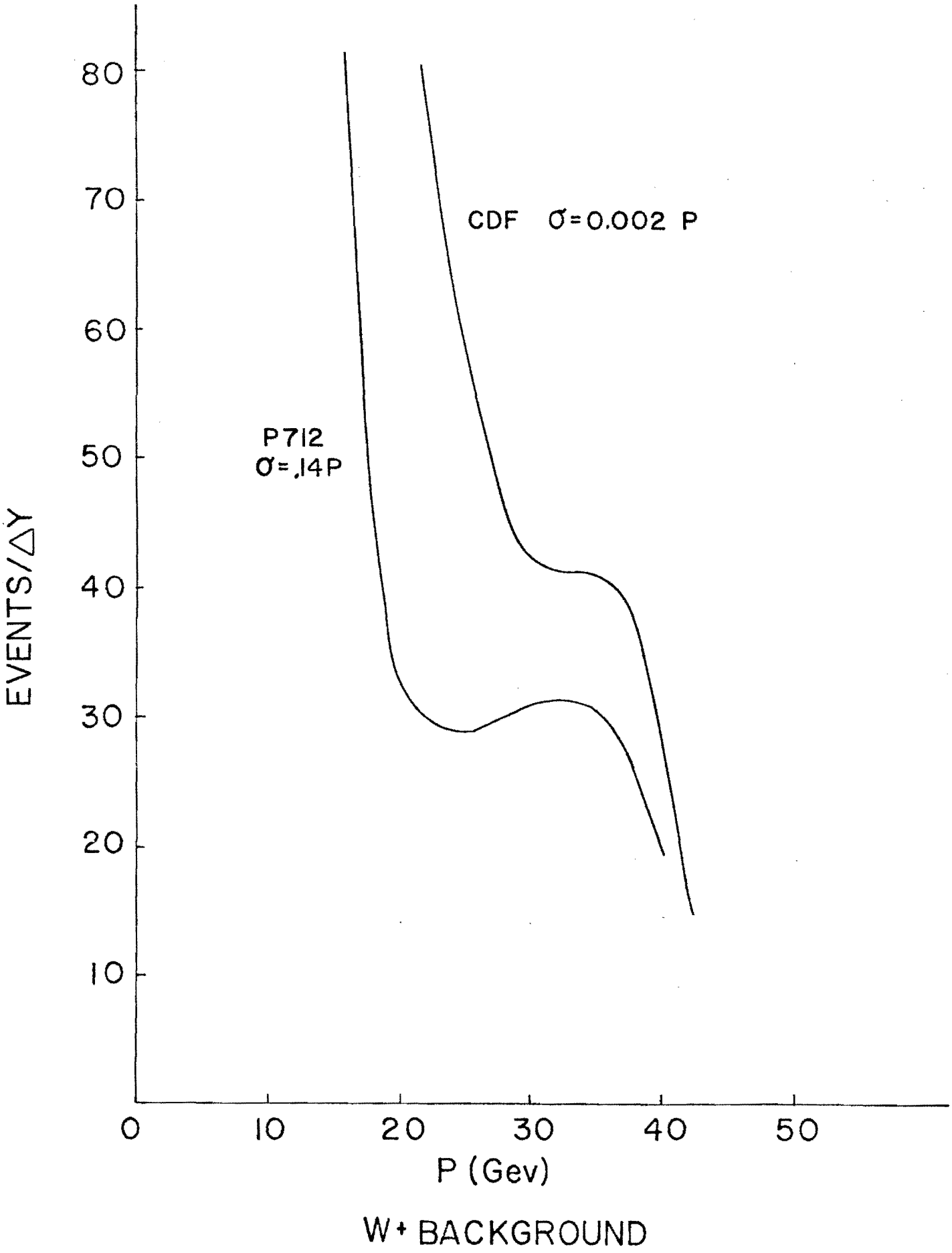
80
70
60
50
40
30
20
10
EVENTS/ΔY
CDF σ=0.002 P
P712
σ=.14P
0
10
20
30
40
50
P (Gev)
W+ BACKGROUND

FIG. 9